Ref. Ares(2023)5772534 - 24/08/2023
Co-funded by the Horizon 2020 programme of the European Union

EMME-CARE

EASTERN MEDITERRANEAN MIDDLE EAST – CLIMATE & ATMOSPHERE RESEARCH CENTRE

HORIZON 2020 – WIDESPREAD-2018-01-TEAMINGPHASE2
EMME-CARE | GRANT NO. 856612

D7.2: Report on health impacts assessment

August 2023

The Cyprus Institute
RESEARCH·TECHNOLOGY·INNOVATION

Max Planck Institute for Chemistry

cea

Helsingin Yliopisto
Helsingfors Universitet
University of Helsinki

This project has received funding from the European Union's Horizon 2020 research and innovation programme under grant agreement No. 856612 and the Cyprus Government

Deliverable Number	Deliverable Title	Lead Beneficiary	Type	Dissemination Level	Due Date (in months)
D7.2	Report on health impacts assessment	MPIC	Report	CO	M48

Version	Date	Changed page(s)	Cause of change	Partner
V1	03/07/2023	Initial version	Added contributions from CARE-C and MPIC	CYI/MPIC
V2	14/07/2023	Final version		CYI/MPIC
V3	August 2023	Final version of D7.2	Final review by the coordinator	CyI

Table of Contents

I. Introduction

I.1. Contribution to WP7

This document is Deliverable D7.2 "***Report on health impacts assessment***" which describes the efforts and outcome of the work of Task 7.2. A brief overview of how this Task is contributing to WP7 "***Impact and Policy Department***" and interconnects with other Tasks and Deliverables of this WP is summarized below.

- **Task 7.1. Creation of an Impact and Policy Department** (Lead: MPG) (M12 -M48)
Status: **Completed**. Submission on M48 of Deliverable D7.1 "***Report on the structure of the Impact and Policy Department***"

- **Task 7.2. Health impact assessment (air quality, climate change)** (Lead: MPG) (M12-M84).
Status: **On-going**. Submission of this Deliverable D7.2 on M48
a. Evaluation of the direct health impact of heat extremes and air pollution (and their combined effects) through high-resolution model-based assessments focusing on urban environments (e.g. urban heat island effect).
b. Evaluation of the indirect health impacts of climate change (linked to water/food security, the spread of vector-borne diseases). Adaptation of models accounting for underlying environmental processes (e.g. vector dynamics), to enable them to be linked to climate models. Investigation of the causes/consequences of severe environmental pressures (possibly leading to migration), in combination with crises, political instability, and armed conflicts.

- **Task 7.3. Methodologies to support implementation of national adaptation plans** (Lead: CyI) (M12-M84). Status: **On-going**. Submission on M48 of Deliverable D7.3 "***Report on methodologies to support implementation of national action plans***"
- **Task 7.4. Impacts on key economic sectors** (Lead: CEA) (M24-M72). Status: **On-going**. Submission on M48 of Deliverable D7.4 "***Report on impacts on key economic sectors***"
- **Task 7.5. Impacts of GHG emission mitigation scenarios** (Lead: CEA) (M36-M84). Status: **On-going**. Submission on M48 of Deliverable D7.5 "***Report on impacts of mitigation scenarios with contribution of EMME and other emitters to the Paris goals***"
- **Task 7.6. Legal framework and policy aspects of (inter)national climate initiatives** (Lead: MPG) (M36-M48). Status: **On-going**. Submission on M84 of Deliverable D7.6 "***Report on legal and policy aspects of (inter)national climate initiatives***"

I.2. Structure and overview

The deliverables described in what follows, are presented in the context of the two types of health assessment (direct and indirect).

For Task 7.2a, the work is presented by type-of-exposure:

Air quality

- The global effect from NO_2 on paediatric asthma was investigated in Section II.1.1
- The assessment of the Covid-19 impact on air quality and the resulting improvement on human health (at global scale but also specifically for Cyprus) (Section II.1.2)
- The potential improvement in human health from better air quality resulting from widespread adoption of a flexitarian diet (Section II.1.3)
- The European health burden from shipping-related air pollution on human mortality was investigated using economic activity models in conjunction with air quality models (Section II.1.4)

- The disease burden from coal-fired power plant emissions in Europe was quantified in terms of excess mortality (Section II.1.5)
- The disease burden from carbonaceous aerosols across Europe was estimated, using an atmospheric chemistry model and well-established exposure-response transfer functions (Section II.1.6)

Heat stress

- Climate data from the CMIP6 experiment were used to project heat-related mortality for the Middle East and North Africa (MENA) region using region-specific heat thresholds, indicating severe increase in mortality risk under all climate change scenarios (Section II.2.1).
- In addition, an artificial intelligence method was developed to quantify the short-term effects of heat-stress, air-quality but also their explicit combination on human health metrics such as mortality and morbidity. This was applied to two case studies, Cyprus and the city of Thessaloniki, Greece, both of which indicated statistically significant increased health risk from poor air pollutions and extreme heat-stress (Section II.2.2).

For Task 7.2b, the work is presented as follow:

- Summary of the current understanding of the effect on human health from Mediterranean Cyclones. To this end, a review paper was published detailing both direct (temperature) and indirect (food security, wind- and dust-storms) effects of these cyclones on physical and mental health (Section III.1).
- Furthermore, machine learning methods have been employed using data from Europe and the USA, to globally project changes in habitat suitability of the Asian Tiger Mosquito (a well-known disease vector), which suggest increased future risk (Section III.2 and III.3.)
- The habitat suitability was further investigated using dynamical models for better physical justification of the projections, further identifying future habitat hotspots over Europe and North America (Section III.4)
- Furthermore, a new mathematical modelling framework for the evolution of mosquito species as a function of climate variables was developed for even more accurate risk projections. (Section III.5)
- Finally, a summary is provided into how EMME-CARE expertise is providing input for an international initiative looking into climate change, human migration and conflict, and eventually public health and wellbeing in the broader Mediterranean region. (Section III.6)

II. Direct health impacts from heat-related extremes and air pollution (Task 7.2a)

II.1. Air quality

II.1.1. Paediatric asthma from NO_2 air pollution

We used ground-based and satellite data, as well as modelling tools, to study the global burden of paediatric asthma from major sources of NO_2. The global new asthma incidence among children attributable to NO_2 was estimated by deriving an exposure-response function from a meta-analysis which included epidemiological studies from multiple countries, baseline incidence rates from the Global Burden of Disease and gridded population data. The sector specific contribution to paediatric asthma from NO_2 exposure was estimated for different source categories to provide guidance to mitigation policies. We find that emissions from land transportation are the largest contributor to new asthma incidence, followed by the domestic burning of solid fuels and power generation from fossil fuels. While only 5% of all children live in areas where NO_2 exceeds the WHO annual guideline for NO_2, about 90% of the new asthma incidence is found in regions that meet the WHO guideline, related to the uneven distribution of children in the population. This suggests the need for improved protection of paediatric asthmatics against NO_2 exposure, and revisiting the current WHO guideline to reduce the health risks of children.

This work was published in Environmental Research Letters (Chowdhury et al., 2021) **"***Global and national assessment of the incidence of asthma in children and adolescents from major sources of ambient NO_2*" (https://doi.org/10.1088/1748-9326/abe909).

II.1.2. Covid-19 impact on air quality

The COVID-19 pandemic has brought unprecedented challenges, which also mobilized new scientific activity, not originally planned under EMME-CARE. We used space-borne and ground-based data, the latter from a network of more than 10,000 measurement stations in 34 countries, to derive atmospheric composition changes during COVID-19 related lockdowns. After accounting for meteorological variability, we found reductions in air pollution concentrations of NO_2 and fine particulate matter of about 60% and 30%, respectively. By incorporating Google and Apple mobility information, the decline of land transport was identified as the main cause of these reductions. Short-term air quality health benefits included the prevention of nearly 50,000 premature deaths and 90,000 paediatric asthma emergency room visits. **This work was published in three (3) peer-reviewed publications:**

1) *Venter et al. (2020)* "Air pollution declines during COVID-19 lockdowns mitigate the global health burden" (https://doi.org/10.1016/j.envres.2020.110403)
2) *Venter et al. (2021)* "Air pollution declines during COVID-19 lockdowns mitigate the global health burden" (https://doi.org/10.1016/j.envres.2020.110403)
3) *Lelieveld et al. (2020*; "Model Calculations of Aerosol Transmission and Infection Risk of COVID-19 in Indoor Environments"; https://doi.org/10.3390/ijerph17218114),

In Lelieveld et al. (2020), we developed a user-friendly model in to estimate the COVID-19 infection risk for different indoor environments, constrained by published data on human aerosol emissions, viral loads, infective dose, and other parameters. The results suggest that aerosols from highly infective subjects can effectively transmit COVID-19 in indoor environments. We showed that active room ventilation and the ubiquitous wearing of face masks (i.e. by all present) can reduce the individual infection risk by a factor of five to ten, similar to highly efficient particle filtering devices.

The impact (benefit) of the COVID-19 lockdown on Air Quality was further evaluated in Cyprus (Nicosia) and reported widely (see WP5).

II.1.3. Co-benefits of a flexitarian diet for air quality and human health in Europe

Agriculture is a major source of air pollution in Europe, with adverse impacts on human health. Having recognised the serious health outcomes, and in direct response to public demand for a cleaner environment, European public policies are aiming to reduce air pollution. In the following we present in details **results of a peer-review publication** (Himics et al., 2022 "Co-benefits of a flexitarian diet for air quality and human health in Europe; https://doi.org/10.1016/j.ecolecon.2021.107232), which focused on a shift to more plant-based human diets to help achieve bold reduction targets for air pollution from agriculture.

Having recognised this regulatory ineffectiveness, the Clean Air Programme for Europe (COM(2013) 918 final) introduced new policy measures to improve the situation. Its main legislative instrument, the new National Emissions Ceilings Directive 2016/2284/EU, sets NH_3 emissions reduction targets for all EU countries: 6% reduction by 2020 and 19% reduction by 2030, relative to 2005 levels. Moreover, agriculture was one of the focus topics of the Clean Air Forums organised by the European Commission in 2017 and 2019, where decision-makers, stakeholders and experts discussed policy strategies for reducing NH3 emissions from agricultural activities. In May 2021, the European Commission adopted its Zero Pollution Action Plan, a key deliverable of the broader European Green Deal policy initiative, which includes a 55% reduction target for air pollution-related premature deaths. The Action Plan identifies the need for further legislative work to curb NH3 emissions from agriculture.

While the health impacts of dietary changes are widely discussed in the literature, still little is known about the potential links between diet changes and air pollution. We aimed to help fill this knowledge gap by quantifying the impact of adopting a flexitarian diet on agricultural NH_3 emissions, and consequently on outdoor $PM_{2.5}$ pollution and associated premature mortality over Europe. Ammonia emissions from agriculture decrease in all European countries. The total reduction in the EU is about 721 000 tons, which corresponds to around a 33% decline compared to the baseline. In general, countries with sizable NH3 emissions have more potential to reduce them (Figure 1).

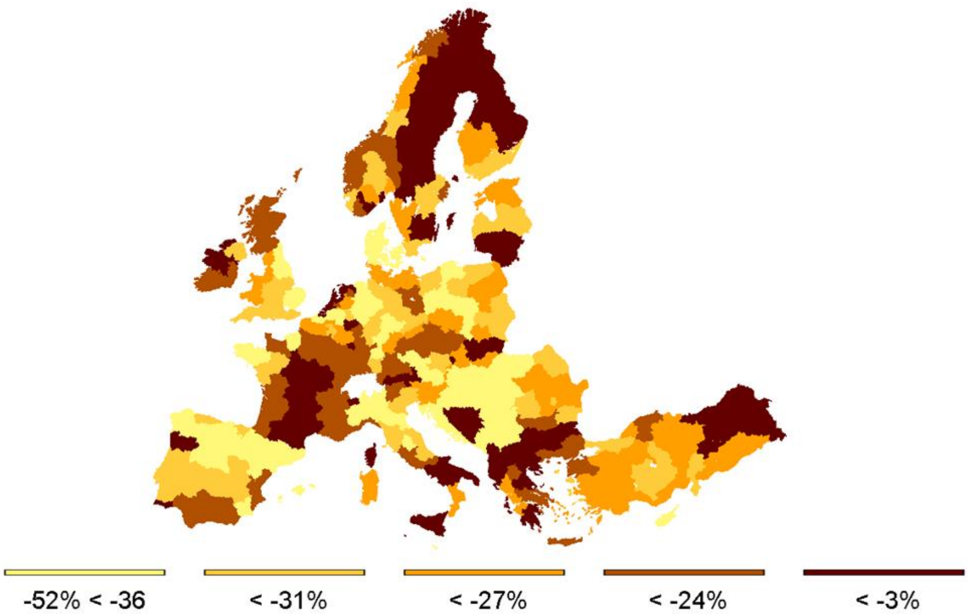

Figure 1: Reduction in ammonia emissions from agriculture, Diet2050 scenario (relative change to baseline, 2050)

Next, we performed an analysis of air quality, with focus on $PM_{2.5}$ concentration as the major contributor to outdoor pollution leading to premature mortality. The modelled mean annual $PM_{2.5}$ surface

concentrations over Europe are presented on an intensity map in Figure 2. $PM_{2.5}$ surface concentrations are shown both for the baseline simulation (in absolute terms) and for the dietary shift scenario (as difference to the baseline simulation results).
Modelled future atmospheric near-surface $PM_{2.5}$ concentrations for 2050 peak over the UK, central Europe, Benelux and Balkan countries at mean annual concentrations reaching 12-14 μg/m^3. Northern Italy and major cities in south-eastern Europe, such as Istanbul, are also among regions with pronounced $PM_{2.5}$ concentrations.

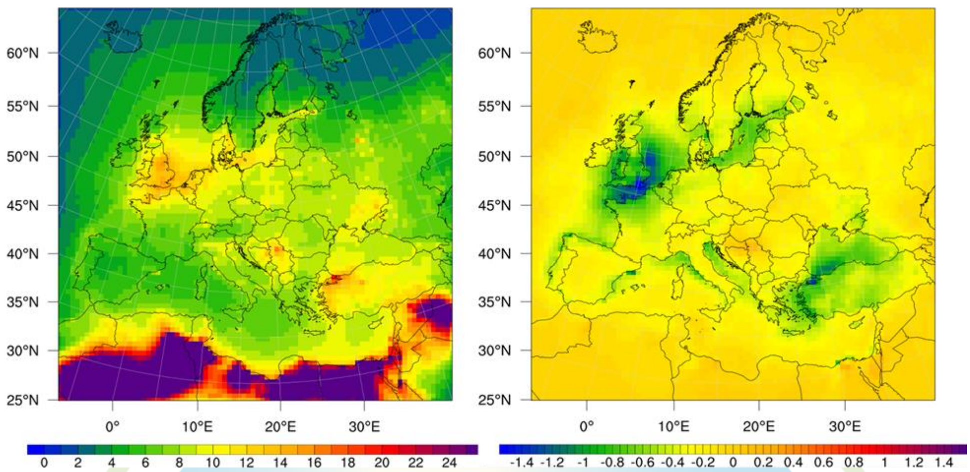

Figure 2. Mean annual $PM_{2.5}$ surface concentrations (μg/m^3) from the 2050 baseline (WCbaseline) simulation (left), and difference in $PM_{2.5}$ concentrations (μg/m^3) between the WCbaseline and dietary shift (WCDiet2050) simulation (right).

The distribution of the differences in near-ground $PM_{2.5}$ concentrations, due to the shift to a flexitarian diet and the subsequent reduction in NH_3 emissions, shows a maximum over the UK and Benelux countries, as well as south-eastern Europe and East Mediterranean, where Cyprus is located. The reduction in surface concentrations peaks at approximately 8% of present $PM_{2.5}$ levels. Next, we quantified the potential health benefits for the region resulting from the reduction in NH_3 emissions (WCDiet2050). Scandinavian countries are the most positively affected, with more than 5% reduction in premature mortality compared to the baseline. The total economic benefits in Europe are estimated at €33 144 million (range: €16 001 m – €50 203 m), with the largest economic benefits found in the UK (€7 999 m) and Germany (€4 552 m). For the EU-27 countries, the total economic benefits amount to €21 948 m. For Cyprus, the economic benefit from reduced mortality (VSL estimate, mean values in euro) reaches €18.2 m with the combined change in producer and consumer surplus and combined monetised health and economic impacts at €21 and €39.2 M respectively.

Summarizing, following a bottom-up approach, we linked simulated ammonia emissions from agriculture (calculated using a partial equilibrium model for the agricultural sector, CAPRI) to related air quality impacts in the atmosphere (calculated using a regional atmospheric chemistry model, WRF-Chem). The 33% average decrease in ammonia emissions in the EU translates into significant air quality improvements over European countries, measured by mean annual PM2.5 surface concentrations. Our results also suggest that the positive health effects from reduced air pollution would largely mitigate the economic losses in the agri-food sector (39% in the EU-27 and 49% in Europe as a whole). Our study focuses on air pollution-related improvements to human health, so this estimate is probably at the lower end of potential economic benefits from a shift to flexitarian diets.

II.1.4. Economic Structure, Air Pollution & Human Health in the EU towards 2030

This work (currently under review at Environment, Development and Sustainability) aims to analyse effects of economic structure on air pollution-related mortality.

Environmentally-extended input-output models and a regional atmospheric chemistry model (WRF-Chem) are combined (EE-IOA) to conduct an economy-wide assessment of air pollution and premature mortality in the European Union (EU) associated with the expected growth of the EU production sectors towards 2030. Model results reveal significant differences in the direct and indirect air pollution intensities of the production sectors across EU countries. Shipping creates the highest air pollutant intensities per unit of economic output. Industry and energy lead to the largest (direct and indirect) increases in near-ground $PM_{2.5}$ concentrations in absolute terms, which are mainly found in central Europe and Scandinavian countries. As a result, the health burden of air pollution is, to a large extent, located in the central and northern part of Europe. The findings of this multi-modelling framework highlight the importance of assessing both direct and indirect emissions from economic sectors via upstream supply chains.

First, through the EE-IOA analysis we identified the contribution of the sixteen (16) economic sectors in the generation (direct and indirect) of air pollution emissions. We found that the maritime transport sector (shipping) generates the largest SOx and NOx pollution intensities. The implication for the maritime transport pollution intensities is that for every million euro increase in the final demand for the products and services of the sector, 7.91 tonnes of SOx and 20.44 tonnes of NOx will be emitted. Shipping also creates the highest $PM_{2.5}$ (1.18) and PM_{10} (1.28) pollution intensities across the EU-28. Agriculture causes the largest direct and indirect NH3 and NMVOC emissions in the EU-28; for every million euro increase in the final demand for the products and services of the sector, 10.36 tonnes of NH3 and 4.60 tonnes of NMVOC will be emitted. Further, the industry and energy sectors have large air pollution (direct and indirect) intensities.

Second, we assessed the increase in $PM_{2.5}$ surface concentrations over Europe due to the increase of the emissions of each of the six top emitting sectors, shown in Figure 3. The industrial, energy and land transport sectors, as expected, due to (a) high emission intensities, (b) large output shares and (c) strong growth rates, lead to the largest increases in near-ground $PM_{2.5}$ concentrations over Europe. Emission changes from air and maritime transport activities, along with agriculture, have a less pronounced impact on surface $PM_{2.5}$ concentrations. For the air transport sector, the maximum influence is distributed across Europe, mostly in countries with major airport hubs of national and international profile. The impacts of emission changes for maritime transport are seen near major sources (coastal areas) but also in locations further downwind. Our results are within the relative impact ranges summarized in Viana et. al (2014) who reviewed the contribution of shipping to $PM_{2.5}$ levels in Europe through various observational and modelling methods.

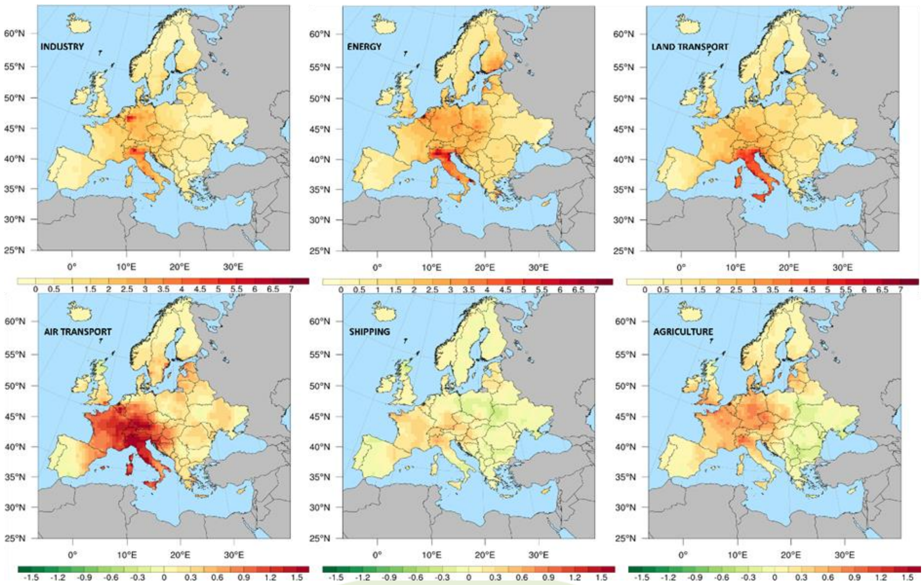

Figure 3. Differences in the mean annual $PM_{2.5}$ surface concentrations (μg/m^3) between the control (CNTR) and the sectoral growth scenarios (INDS2030, ENERG2030, LAND2030, AIR2030, SHIP2030, AGRIC2030) simulations. Note the different colour bars between the top and bottom panels.

Finally, we quantify the health burden for the EU-28 region resulting from the sectoral scenarios (Figure 4). The most strongly affected countries from industrial sectors, with enhanced mortality in excess of 10% compared to the control run, are the Scandinavian countries, Germany and Italy. Similar health effects are also found for the energy sector emission perturbations. Land emissions increases affect countries located in the central part of Europe (France, Italy, Austria, Slovenia, Sweden). For the remainder three sectors, i.e., air transport, shipping and agriculture, the mortality increase is less than 10% compared to the baseline, due to the small size of the sectors in terms of economic output generation.

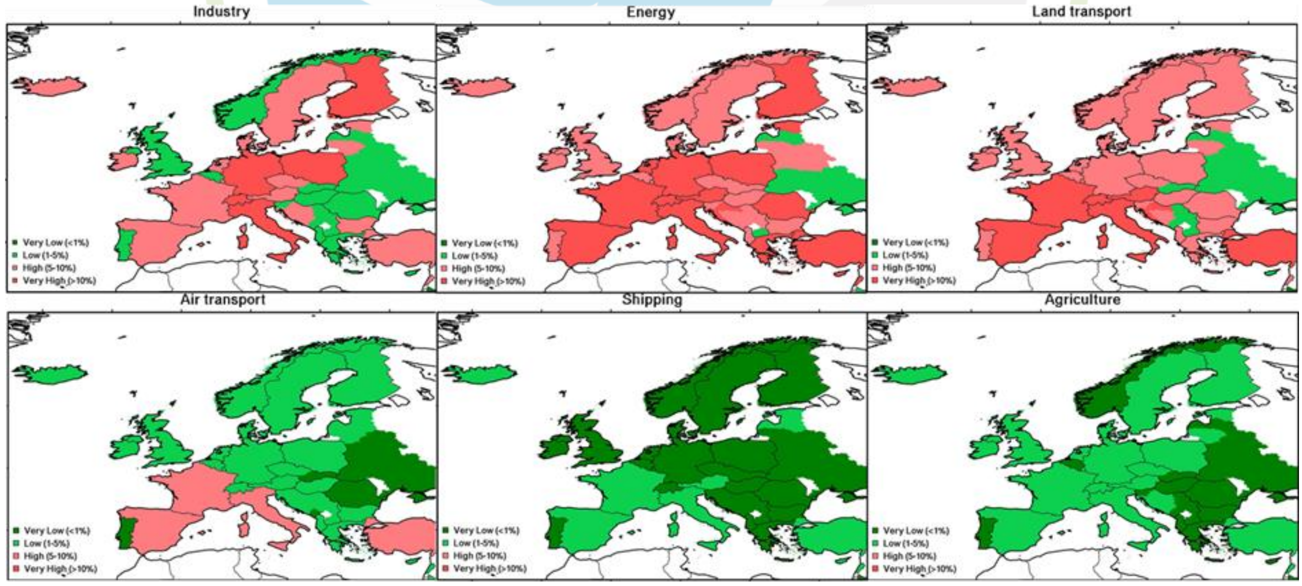

Figure 4. Country-level excess mortality rate estimates in Europe due to outdoor air pollution levels of PM2.5 from the sectoral growth scenarios (INDS2030, ENERG2030, LAND2030, AIR2030, SHIP2030, AGRIC2030) relative to the control PM2.5 concentrations (CNTR), classified into four categories: very high sensitivity (mortality increase >10%), high sensitivity (mortality increase between 5 and 10%), low sensitivity (mortality increase between 1 and 5%) and very low sensitivity < 1%).

Summarizing, despite the fact that the identification and quantification of driving economic factors of air pollution-related mortality are key elements in formulating pollution abatement strategies and policies, remarkably, the effects of economic structure on air pollution and human health have not yet been widely explored. Our results contributed to this knowledge gap with an analysis of how the expected growth of the EU-28 production sectors might affect air pollution and human health in Europe towards 2030.

II.1.5. Disease burden from coal-fired power plant emissions leads to excess mortality in Europe

We studied the contribution of coal-fired power plant (CPP) emissions to excess mortality by cardiovascular and respiratory diseases in Europe for 2015, based on fine particulate matter (PM2.5) concentrations computed with a regional atmospheric model. **This was led to one (1) peer-review publication**: *Kushta et al., (2021)* "Disease burden and excess mortality from coal-fired power plant emissions in Europe" (https://doi.org/10.1088/1748-9326).

Electricity generation using fossil fuels remains a large global contributor to the emissions of aerosol particles and their precursors in the atmosphere. The global electricity generation fuel share of coal power plants was 40.4% in 2012 (IEA, 2014). In the European Union (EU-28) almost half (49.8%) of the network electricity came from power stations using combustible fuels (biomass, natural gas, coal and oil) in 2013. Predominant emissions from fossil fuel combustion are SO_2, NO_x, carbon monoxide (CO), particulate matter (dust and fly ash) and greenhouse gases such as CO_2.

The wide range of hazardous substances emitted by CPPs can affect public health, not only in the vicinity of the power plants, but also at great distance due to long range transport of pollutants through the atmosphere. The Health and Environmental Alliance (HEAL, https://env-health.org/IMG/pdf/dark_cloud-full_report_final.pdf), Climate Action Network (CAN) in Europe, and WWF European Policy Office, estimate that coal related emissions are responsible for 22,900 excess deaths annually based on data from 257 CPPs in Europe with 19,000 due to elevated levels of $PM_{2.5}$, 3,800 from NO_2 and 200 deaths from O_3. This comes at a public health cost of up to €62.3 billion each year. Markandya and Wilkinson (2007) estimated the burden of the health effects of generating electricity from coal in Europe at 24.5 deaths, 225 serious illnesses and 13,288 minor illnesses for every TWh (Terrawatt-hour) of electricity produced from coal. When lignite, (most polluting), is used, each TWh of electricity produced may result in 32.6 deaths, 298 serious illnesses, and 17,676 minor illnesses).

In our study we re-evaluated the relative contribution of CPP emissions over Europe on particulate matter PM levels and consequently on mortality estimates in the EU-28 member states for the year 2015. We perform base case and sensitivity simulations (with and without emissions of gaseous precursor of aerosols, namely SO_2 and NO_x, and primary aerosol emissions $PM_{2.5}$ and black carbon) from 260 CPPs in Europe. We performed simulations with and without CPP emissions and estimated the difference in air quality status and health outcomes.

The annual mean $PM_{2.5}$ concentrations from the simulations were used to estimate excess mortality for a range of related diseases and age groups, based on the integrated exposure-response (IER) functions as described in Burnett et al. (2014). For the calculation of the relative risk (RR) factors, which are key parts of the IERs, we used the updated parameters also used for the global burden of disease (GBD) for 2015 (Cohen et al., 2017). In this study, IER functions were applied to account for health effects of $PM_{2.5}$ related to ischaemic heart disease (IHD), cerebrovascular disease (CEV), lower respiratory tract infections (LRIs), chronic obstructive pulmonary disease (COPD) and lung cancer (LC).

We analyzed the respective burden of disease for the age groups < 5 years, 5-14, 15-29, 30-49, 50-69 and >70 years old.

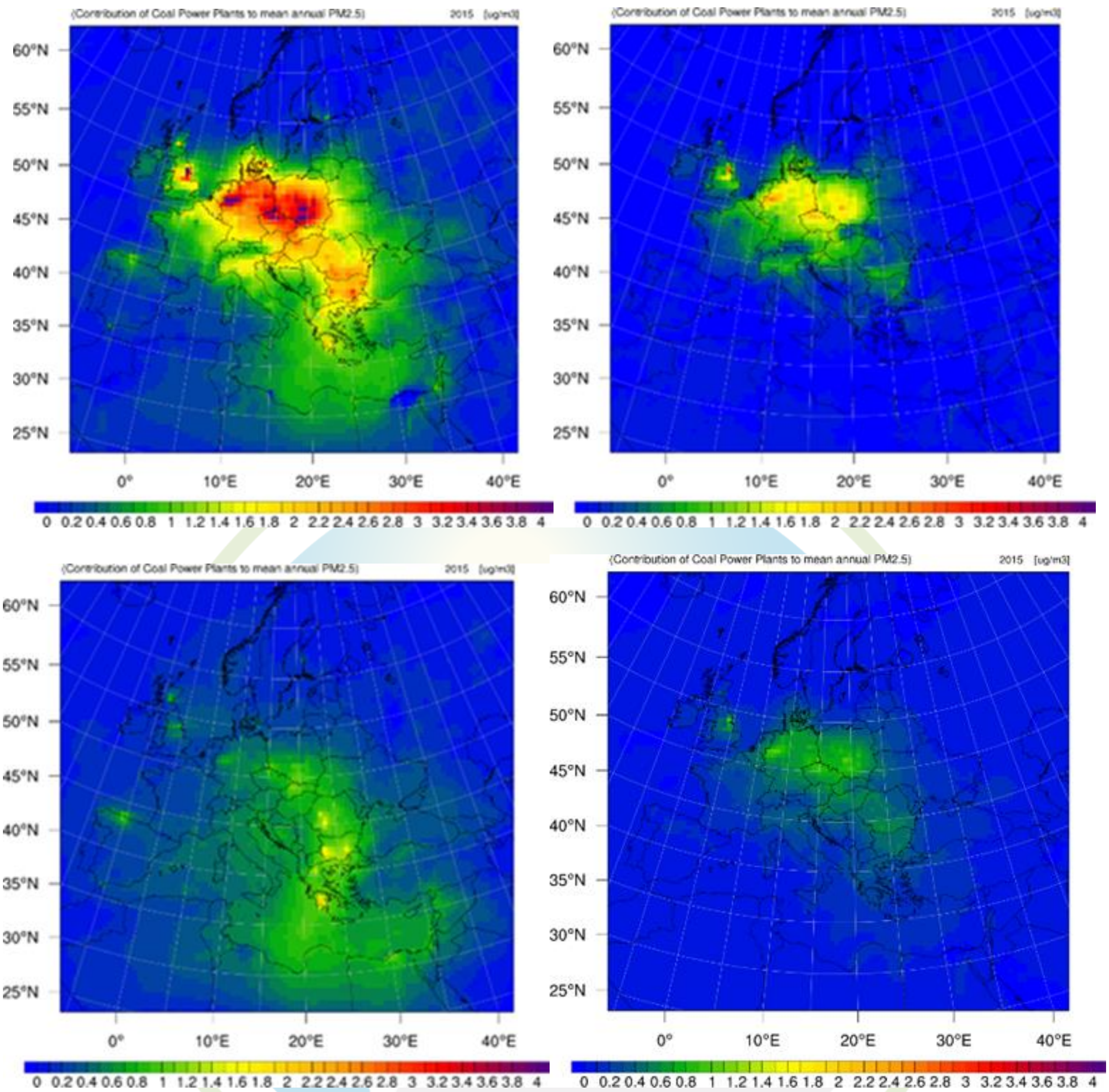

Figure 5. Difference in annual mean concentrations (in µg m-3) for the year 2015 of a) total PM2.5, b) NO3-, c) SO4-2 and d) NH4+ over the model domain expressed as CCOAL-CNOCOAL

The annual mean contribution of CPPs to $PM_{2.5}$ concentrations is 1-4 µg m^{-3}, centered around the major emitters, Germany and Poland (Figure 5). The difference in total $PM_{2.5}$ results from primary and secondary aerosol components. Excluding the CPP emissions mostly influences nitrate levels in the vicinity of the emission sources while the impact of CPPs on the sulphate aerosols is more uniform over all Eastern and South-eastern Europe. The CPP influence on the distribution of emission fluxes of the gaseous pollutants SO_2 and NO_x affects the distribution of the ammonium aerosols with the largest changes following the changes in the nitrate component. The differences in both total $PM_{2.5}$ and aerosols components (nitrate, sulphate and ammonium aerosols) are more pronounced in areas where the changes are driven by the nitrate component.

We then calculated the total excess mortality rates from the aforementioned diseases, for the EU-28 member states for the base case and the two sensitivity tests expressed as the annual total mortality rate per 100,000 inhabitants and total excess deaths due to the emissions from CPPs. We further integrated the net electric capacity of the CPP units excluded from the emission inventory per EU-28 member state, and calculated a benefit index (BI) as the number of excess deaths due to emissions from the CPPs of that country to the net capacity of the CPPs. This parameter is a measure of the gain per country when clean electricity production replaces the use of coal in Europe. This number however must not be taken as a measure of national achievement, as the reduction in excess mortality in each country is not a result of the reduction of the respective emissions from that country alone, but rather a collective effort from all EU-28 member states. Further, it cannot be used as a 'cost-benefit' index as this ratio is strongly influenced by the non-linearity of the relationship between national coal power plant productivity and excess mortality due to the transboundary transport of pollution. Countries without CPPs or when information was absent or not accessible are stated as 'No CPPs excluded'. In these countries the excess deaths are only a result of the emissions from neighboring and further upwind countries.

As shown in Figure 6 (7 categories of benefit index), Austria, Belgium, Croatia, Hungary and Slovakia will have the largest benefit in terms of fewer excess mortality relative to the electricity range they decarbonize from coal (>0.5). On the other hand, Denmark, Finland, the Netherlands, Slovenia and Spain will have the smallest reductions in excess mortality relative to the total electricity potential needed to be replaced by other sustainable and less polluting fuels. This occurs when either the national coal-related emissions are small, or when the country is not affected by large upwind CPP emitters.

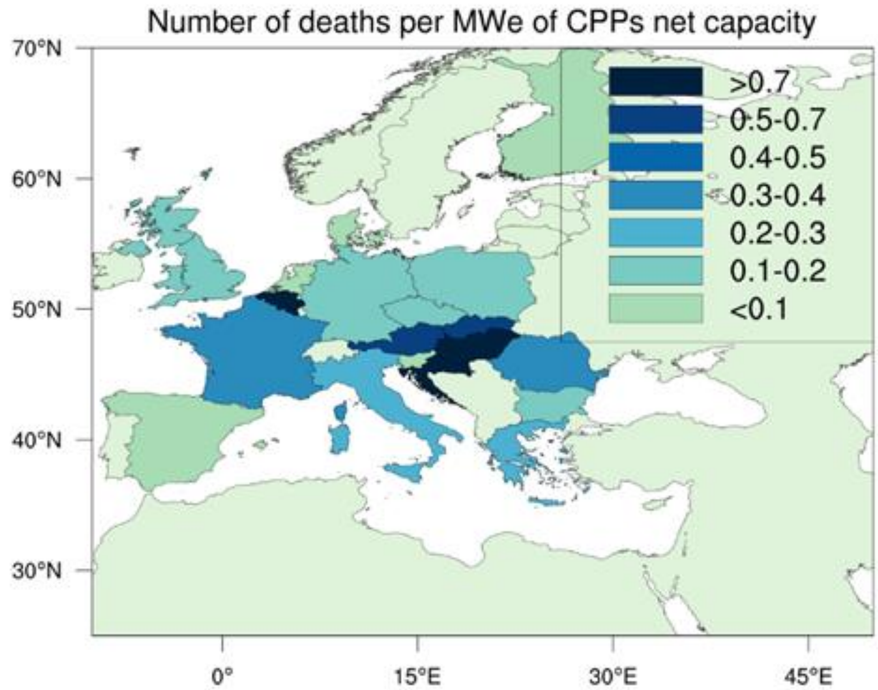

Figure 6. Benefit index expressed as number of excess deaths that can be avoided per electricity power unit (MWe) produced from coal power plants per country in the EU-28

We compared the results of this study with the results of Markandya and Wilkinson (2007) by assessing the gross electricity production over Europe, for each fuel type (separate value for coal) from the EEA (https://www.eea.europa.eu/data-and-maps/indicators/overview-of-the-electricity-production-1/assessment). In 2010 the gross electricity production from CPPs in the EU-28 member states was 818.4 TWh, therefore the health burden from generating electricity with coal reaches 19.8 - 25.8 deaths per TWh of produced electricity (based on the emission reduction approach, confidence interval 17.5 – 21.6 for the first approach and 22.7 – 28.1 for the second approach), consistent with the 24.5 deaths reported in Markandaya and Wilkinson (2007) for coal. Due to the non-linearity of the integrated response functions, if simultaneous pollution control strategies are applied to other sectors of anthropogenic activities then approx. 51,000 lives can be saved each year by phasing out CPP units in the EU-28 member states. The mortality rates per 100,000 inhabitants under a coordinated and simultaneous emission control strategy would drop significantly in all countries by about 50 – 80%. This health burden should be taken into account when discussing the necessity and urgency of phasing out coal from the electrical power sector.

II.1.6. Carbonaceous aerosols and their health impacts

Epidemiological and toxicological studies have strong evidence that carbonaceous particles (black carbon and organic aerosols), especially secondary organics from combustion sources, are more hazardous to human health than other inorganic ones. Health impact studies and emission reduction policies are based on total $PM_{2.5}$ concentration without differentiating the more harmful components.

In the framework of EMME-CARE (Task 7.2.a), we used the Weather Research and Forecasting model coupled online with chemistry (WRF-Chem) to simulate ambient $PM_{2.5}$ concentrations over the wider European domain and have assessed some of the main factors that contribute to uncertainty (Paisi et al., 2023). In particular, we explored the impact of anthropogenic emissions and meteorological modeling on carbonaceous aerosol concentrations with several sensitivity tests. We further used the Global Exposure Mortality Model (GEMM) by Burnet et al. (2018), to estimate excess mortality from exposure to $PM_{2.5}$, the contribution of anthropogenic carbonaceous aerosols and the role of the main uncertainty factors on the excess mortality estimates.

Overall, the modeled $PM_{2.5}$ and black carbon (BC) concentrations agreed with ground-based observations in all simulations, however, organic aerosols showed a systematic negative bias, that ranged between -69% and -50% depending on the configuration (Figure 7). These modeling uncertainties related to organic aerosols lead to a ~13% deviation in excess mortality due to $PM_{2.5}$ in Europe (Figure 8). The simulation with default model configuration resulted in a total of 680 (95% confidence interval 558-802) annual excess deaths over Europe, whereas the best-performing model configuration in 770 (CI: 632-906). Accordingly, the population-weighted excess mortality was estimated to be 128 and 138 excess deaths per 100.000 population per year respectively. The difference in population-normalized excess mortality due to anthropogenic carbonaceous aerosols between the default and best-performing simulations showed to be relatively small (on average 15 and 23 deaths per 100,000 individuals per year. However, these differences due to modeling uncertainties are relevant when all $PM_{2.5}$ sub-components are assumed to be equally toxic. The difference is expected to be higher when their differential harmfulness on health is considered.

Additional sensitivity tests on differential toxicity were performed, where we assumed that anthropogenic carbonaceous aerosols are two and five times more toxic than other fine particles. While anthropogenic carbonaceous aerosols contributed to ~12% of the total excess mortality when equal toxicity was assumed (with the best-performing simulation), this fraction increased to 25% and 69% of the total when anthropogenic carbonaceous aerosols were considered to be two and five times more toxic, respectively. These fractions equal to 35 and 95 annual excess deaths per 100.000 people respectively.

The results have a strong dependence on the shape of the hazard ratio model used (i.e. GEMM), which drives the relationship between $PM_{2.5}$ concentration and mortality risk. However, we expect that the uncertainties in organic aerosols modeling will have a greater impact on studies in which the relatively high harmfulness of carbonaceous aerosols is accounted for. Improving the modeling of this category of particles is of particular importance for health impact studies that focus on smaller domains (e.g., at national or municipal level), and include differential toxicity information of carbonaceous fine particles. Explicit account and reporting of organic precursors (SVOCs/IVOCs) in all emission inventories would improve the accuracy of organic aerosols modeling and subsequently the relevant health impact/health benefit analysis.

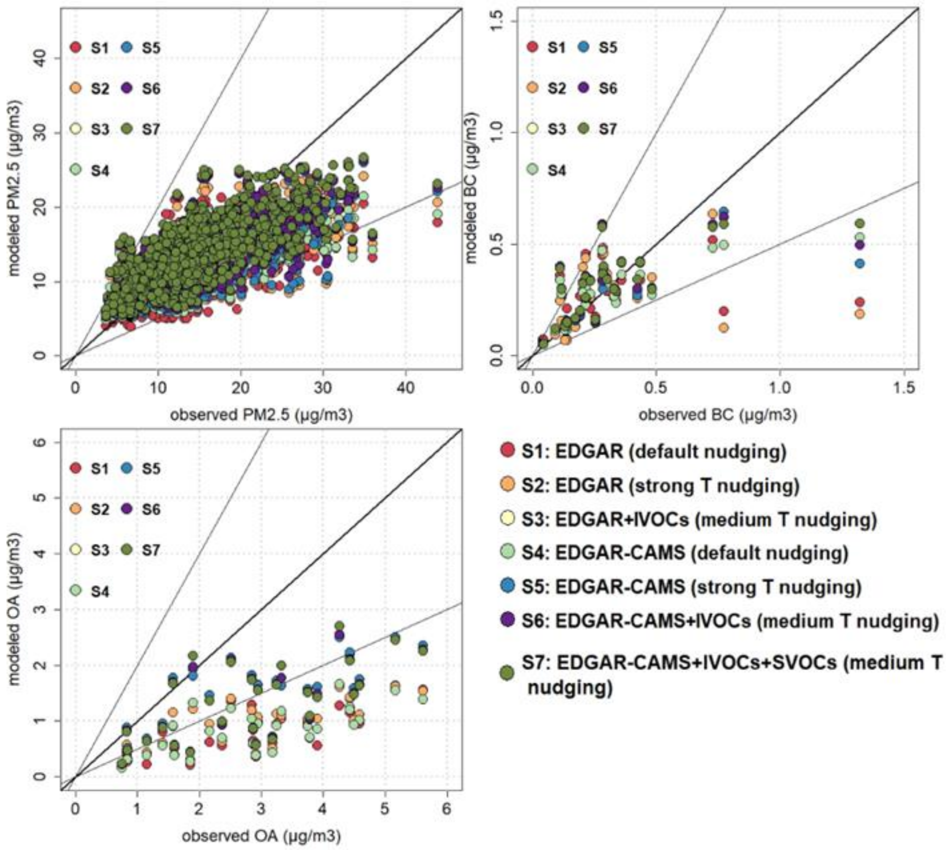

Figure 7: Annual modeled $PM_{2.5}$, black carbon, and organic aerosols compared to observations.

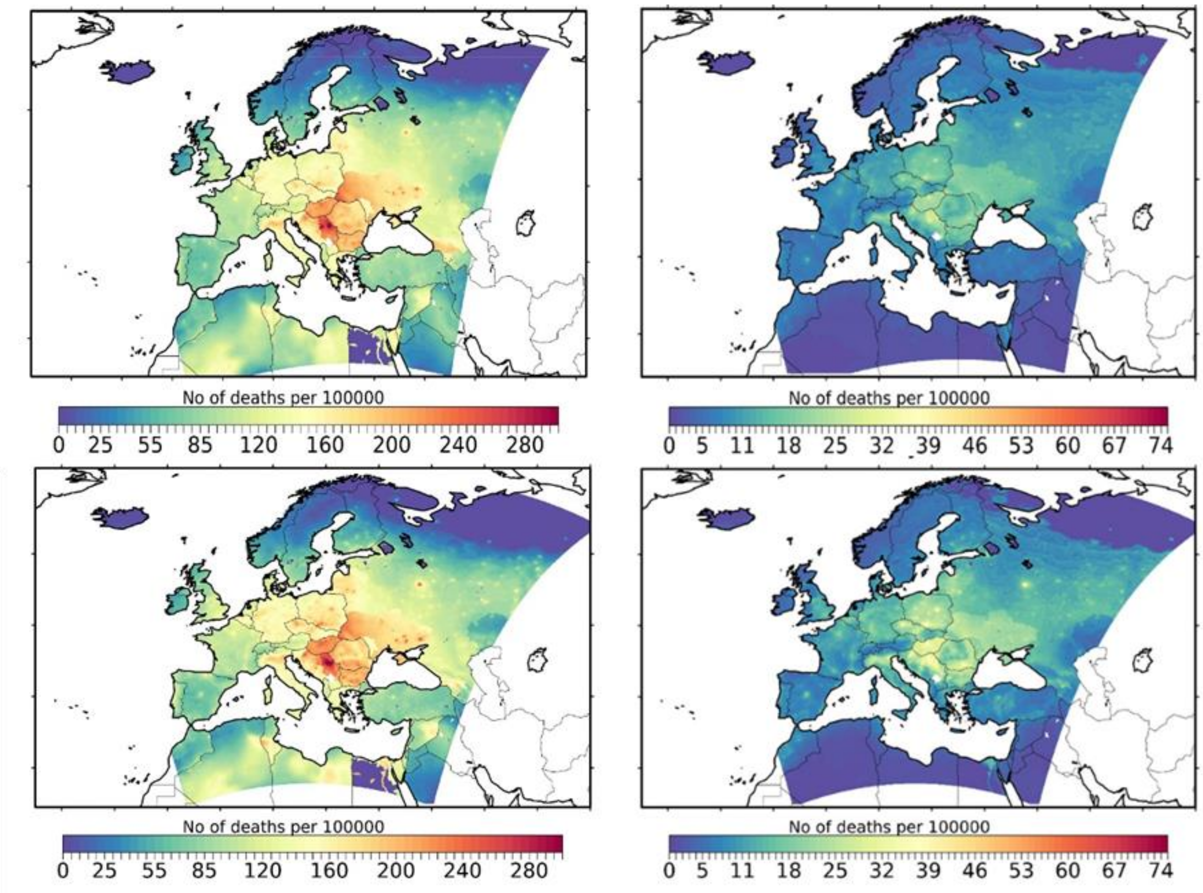

Figure 8: Annual excess mortality normalized to the population in each grid cell (20 km horizontal resolution) due to $PM_{2.5}$ (left panels) and anthropogenic carbonaceous aerosols (right panels) estimated by the default (upper panels) and best-performing (bottom panels) simulations.

II.2. Heat-stress

II.2.1. Heat related mortality projections for the MENA region

Leveraging global climate projection datasets from the latest Coupled Model Intercomparison Project (CMIP6) that encompass four different warming scenarios (i.e., SSP1-2.6, SSP2-4.5, SSP3-7.0, and SSP5-8.5), we have developed state-of-the-art biased adjusted and statistically disaggregated datasets to study the combined effects of near-surface temperature and relative humidity on heat-attributed mortality. Through the utilization of an epidemiological model, we have focused on selected countries within the Middle East and North Africa (MENA) region and made projections for the heat-mortality rates for the period spanning 2015 to 2100.

The findings of this extensive modelling study on heat-related mortality, have been published in The Lancet Planetary Health journal (*Hajat et al., 2023*) “Current and future trends in heat-related mortality in the MENA region: a health impact assessment with bias-adjusted statistically downscaled CMIP6 (SSP-based) data and Bayesian inference” (https://doi.org/10.1016/S2542-5196(23)00045-1).

In summary, our study reveals that constraining global warming to 2°C could avert over 80% of projected heat-related deaths in the MENA domain by the end of the century (e.g., see Figure 9a, which depicts the relative change in annual heat-related mortality rates for future periods compared to the baseline period (2001–2020)). In addition, temporal trends in annual heat-related mortality up to the end of the century under each SSP (Shared Socioeconomic Pathways) scenario based on the GAM (Generalized Additive Models) statistical analysis are shown in Figure 9b, where the time-series plots for each MENA country considered in the study are arranged in ascending order in terms of the mortality magnitude. It is evident, that the MENA region is highly susceptible to the adverse and profound impacts of climate change, and scenarios characterized by high greenhouse gas emissions project a substantial increase in heat-related mortality. Despite this amplified vulnerability, the impact of heat stress on human population in the region remains underexplored (mainly due to the lack of epidemiological data). Urgent action is imperative to implement improved adaptation policies, and actionable practices that will allow a swift transition to renewable energy technologies. With the forthcoming COP28 in Dubai, a pivotal opportunity arises to address this pressing issue. It is crucial to formulate and develop alternative strategies beyond the conventional heat-adaptation measures such as air-conditioning and strengthen health systems to safeguard citizens from the consequences of the extreme and prolonged heat events in the region.

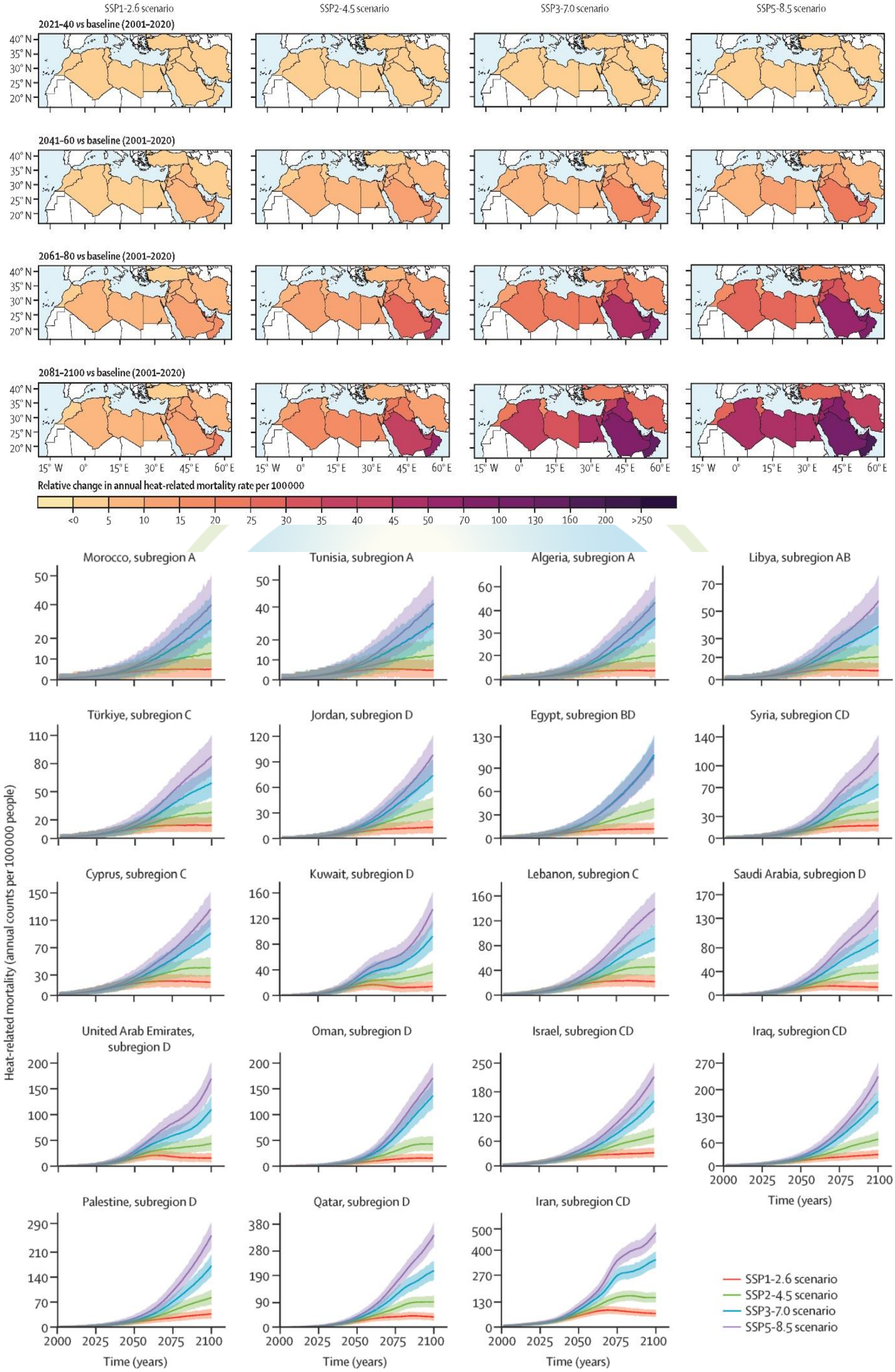
SSP1-2.6 scenario
SSP2-4.5 scenario
SSP3-7.0 scenario
SSP5-8.5 scenario
2021–40 vs baseline (2001–2020)
2041–60 vs baseline (2001–2020)
2061–80 vs baseline (2001–2020)
2081–2100 vs baseline (2001–2020)
40° N
35° N
30° N
25° N
20° N
15° W
0°
15° E
30° E
45° E
60° E
Relative change in annual heat-related mortality rate per 100 000
<0
5
10
15
20
25
30
35
40
45
50
70
100
130
160
200
>250
Morocco, subregion A
Tunisia, subregion A
Algeria, subregion A
Libya, subregion AB
Türkiye, subregion C
Jordan, subregion D
Egypt, subregion BD
Syria, subregion CD
Cyprus, subregion C
Kuwait, subregion D
Lebanon, subregion C
Saudi Arabia, subregion D
United Arab Emirates, subregion D
Oman, subregion D
Israel, subregion CD
Iraq, subregion CD
Palestine, subregion D
Qatar, subregion D
Iran, subregion CD
Heat-related mortality (annual counts per 100 000 people)
Time (years)
2000
2025
2050
2075
2100
SSP1-2.6 scenario
SSP2-4.5 scenario
SSP3-7.0 scenario
SSP5-8.5 scenario

Figure 9: a) Relative change in annual heat-related mortality rate (per 100 000 population) for each country with respect to the baseline period 2001–2020. Each column corresponds to a different CMIP6 SSP projection scenario for four different 20-year periods (2021–2040, 2041–2060, 2061–2080, and 2081–2100). b) Annual total projections of heat-related mortality risk in each country for the four CMIP6 SSP pathways over the period 2001–2100. The lines are fit based on the statistical GAM model applied to the computed heat-related mortality risk, and the shaded areas represent the associated uncertainty expressed as 95% prediction intervals. The ***plots are arranged in ascending order in terms of impact***, with a different scale on the y-axis in each case. [CMIP6=Coupled Model Intercomparison Project phase 6. GAM=Generalised Additive Model. SSP=Shared Socioeconomic Pathway. SSP1-2.6=consistent with a 2°C global warming scenario. SSP2-4.5=medium pathway scenario. SSP3-7.0=pessimistic scenario. SSP5-8.5=high emissions scenario].

II.2.2. Artificial intelligence methods to quantify synergetic health impacts

The direct health impacts from either heat stress or poor air quality are relatively well-understood. Their synergistic effect, however, is not as well documented, primarily due to the lack of available statistical methodology. To understand the health effects from different stressors over several days, we have developed a novel statistical framework based on hierarchical Bayesian models. Specifically, the data modelling framework can be used to quantify the association between daily mortality/morbidity and stressors such as heat and air quality, and the way that this association is distributed over several days (lags). The statistical model can capture the synergistic effects of any number of stressors over several days, on any health outcome. **A paper on the framework is being submitted to Proceedings of the Royal Society A.**

The new framework has been applied to data from Cyprus to investigate the effects of temperature and relative humidity on human mortality. The findings were somewhat surprising (Figure 10) in that the temperature-related mortality risk was much higher for low temperatures and high relative humidity, likely due to the adaptation of the Cyprus population to heat stress and the transmission of viruses during the winter months. **A paper is in preparation for Environmental Health.**

The framework was also applied to data from the city of Thessaloniki, Greece, to study the synergy between heat and air quality. The results indicate that heat-related mortality is exacerbated by poor air quality, particularly with high PM_{10} levels, but also Ozone and nitrogen dioxide (Figure 11). **A paper is in preparation for the Lancet Regional Health**. A similar study was performed for Cyprus, which confirmed the negative interaction between heat and poor air quality in terms of mortality.

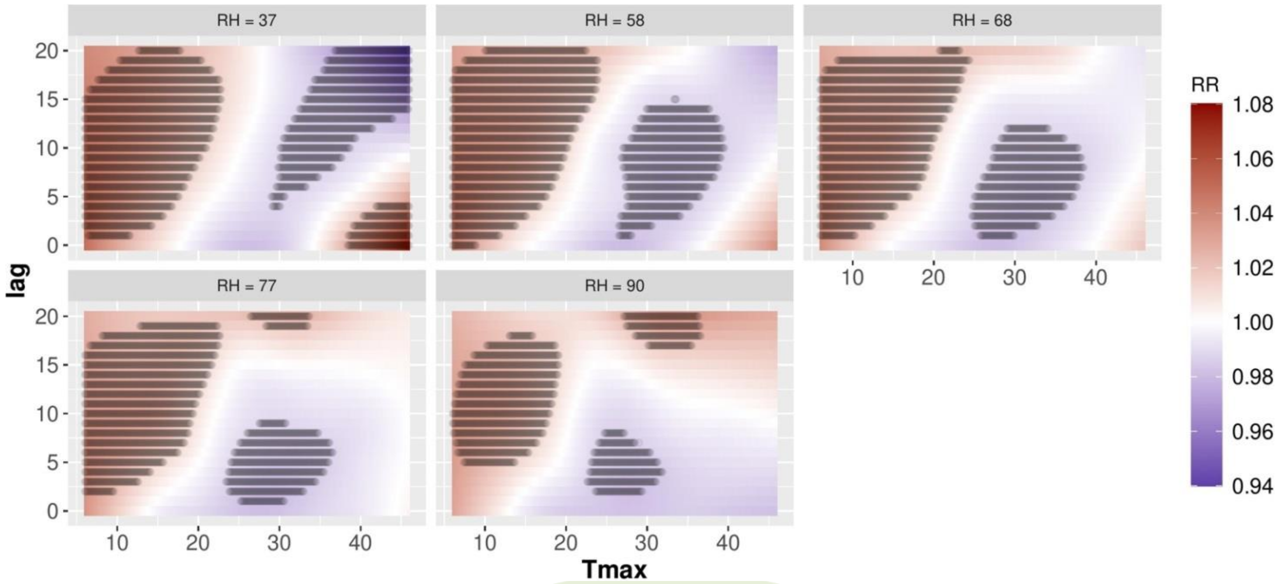

Figure 10: Synergistic effects of maximum temperature and relative humidity on human mortality for Cyprus. The plots are in increasing values of relative humidiy. The x-axis relates to temperature values, the y-axis is the temporal lag (up to 20 days) while the colour relates to risk: red/blue colour indicates higher/lower mortality risk than average.

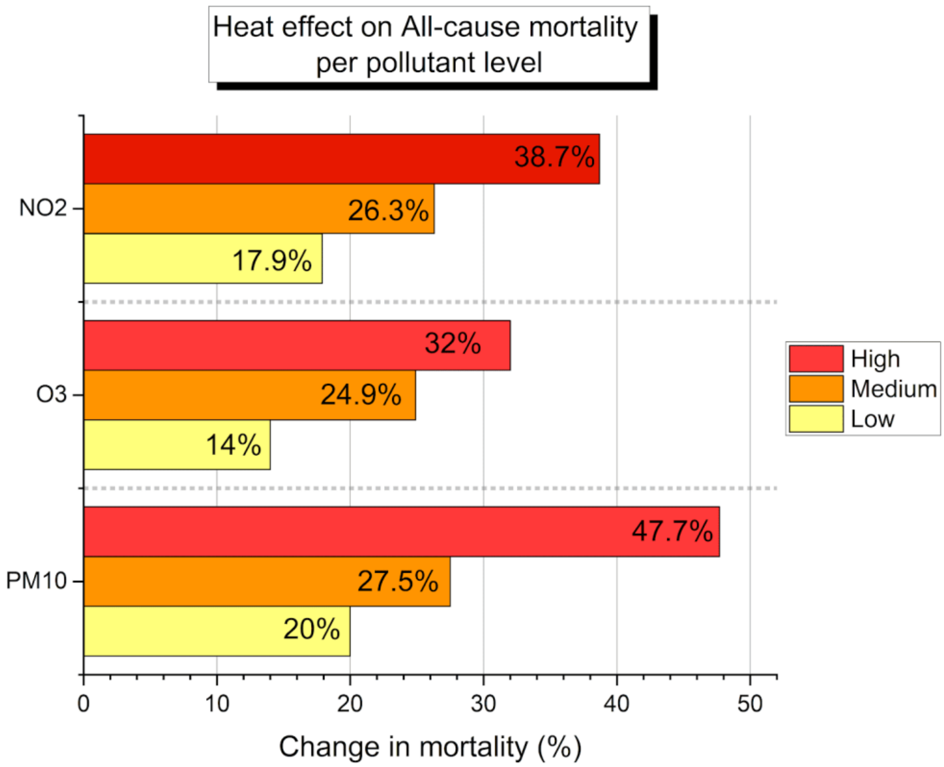

Figure 11: Synergistic effects between extreme high maximum apparent temperature and top) nitrogen dioxide, middle) Ozone and bottom) particulate matter of 10 microns or less, for Thessaloniki, Greece. The x-axis is the percentage change in mortality risk (number of deaths), which is stratified by low, medium and high levels of each pollutant.

III. Indirect health impacts from climate change (Task 7.2b)

III.1. Mediterranean Cyclones and Human Health

Climatic changes impact the heath of the global and Mediterranean population directly through extreme heat, drought or storms, or indirectly by changes in water availability, food provision and quality, air pollution, spread of vector-borne diseases and other stressors. Besides the exposure to harsh weather conditions, these impacts strongly rely on socioeconomic and demographic factors such as age, gender, the existence of pre-existing or chronic diseases, geographic location, level of acclimatization, occupational health and safety, quality of health services and more.

Victims of extreme weather events and hydrogeological hazards (e.g., floods, landslides and windstorms), particularly when accompanied by casualties and property losses, are more subject to short- or long-term mental illnesses and disorders, including depression, anxiety or post-traumatic stress disorders. However, several methodological challenges arise when conducting studies on the psychosocial and mental health impacts of such events, while there is limited research for the Mediterranean region.

While the direct physical health impacts of MedCyclones and associated extreme weather are well-understood, the mental health impacts of such events under a changing climate remain an under-researched field internationally and regionally in the Mediterranean (Figure 12). In the framework of the MedCyclones COST Action (https://medcyclones.eu/), **we have contributed to a review paper** (*Hatzaki et al., 2023*) “MedCyclones: Working Together toward Understanding Mediterranean Cyclones” (https://doi.org/10.1175/BAMS-D-22-0280.1).
This paper aims to assess the existing knowledge and identify research gaps regarding the socio-economic impacts of Mediterranean cyclones with a focus on vulnerable sectors, such as human health (Khodayar et al., 2023). The main findings are summarized in the following paragraphs.

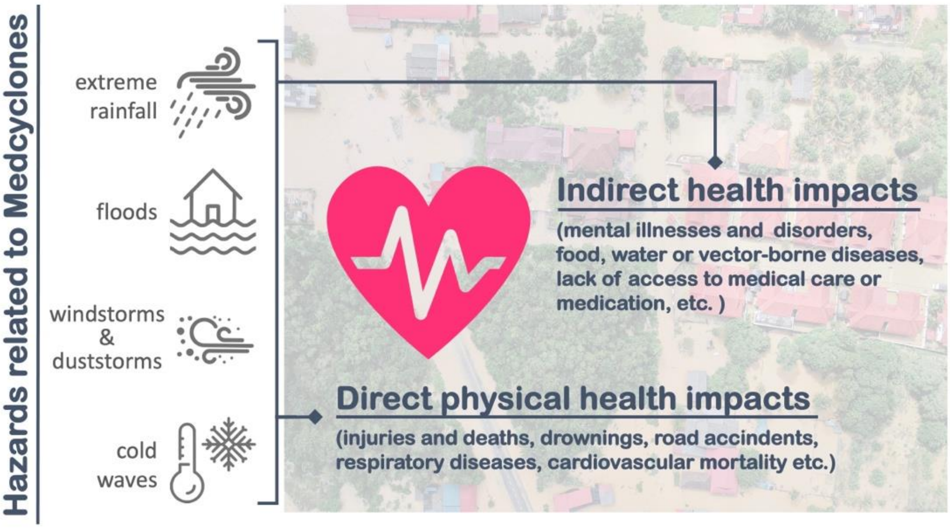

Figure 12. Graphical summary of the meteorological hazards related to Mediterranean Cyclones and their impacts on human health.

Food security and Agriculture: Agriculture and water are closely interlinked in Mediterranean countries and shape the social development in many rural areas. Nevertheless, most of the countries within the region are net importers of cereal and fodder/feeding products, so any further environmental stresses on agriculture production, including climate change and extreme events, will pose additional challenges for food security. In addition, socio-economic and demographic factors (e.g., changes in dietary patterns, population growth or import/export flows) will also impact the regional demand for food. A prime impact of food insecurity is malnourishment leading to malnutrition, which refers to deficiencies, excesses, or imbalances in a person's intake of energy and/or nutrients. Malnutrition is already an issue in some northern African and eastern Mediterranean countries, with a significant portion of their population characterized as stunting, wasting or underweight.

Mediterranean cyclones provide most of the wet-season rainfall, which is critical for replenishing water resources and beneficial for agriculture and ecosystems. However, the most extreme events, associated with severe winds, intense rainfall and flooding, can be a threat for plants and agriculture production. For example, extreme amounts of precipitation and water excess in the soil can be responsible for wheat loss due to the proliferation of pests and diseases, leakage of nutrients, inhibition of oxygen uptake by roots, and interference with agronomical practices. In a hotter and drier Mediterranean, the yield and quality of several key crops for the region, including cereals, vegetables, pulses, grapevines and olive trees, will be adversely affected, with the impacts being more pronounced in the water-stressed southern and eastern Mediterranean countries. Additional risks will be posed during the most severe extreme events. The agriculture sector will need to promptly and efficiently adapt to tackle the climate-induced challenges of future crop production and meet the increasing food demand of the growing regional population. While the impact of mean climate change in agriculture and the role of droughts and heat extremes have been widely investigated, the effect of extreme precipitation events on future crop yields is less studied. In addition, more research is required to fully comprehend the synergies and trade-offs within the regional food-water-energy nexus and identify any potential health implications under a changing climate.

Windstorms and Dust storms: The strongest windstorms in the Mediterranean are often associated with a cyclone. The health impact of such events can be divided into direct and indirect. Direct effects occur during the impact phase of a storm, causing deaths and injuries due to the force of the wind (e.g., from flying debris, falling trees or road accidents), while the indirect effects mostly occur during the post-impact phases of the storm (e.g., power outages that can lead to electrocution, fires and burns, worsening of chronic illnesses due to lack of access to medical care or medication). Extreme winds can also contribute to the rapid spread of forest fires and create hazardous conditions for sailing, maritime shipping and aviation. On average, the mean future conditions imply a decrease in the frequency and intensity of windstorms; however, the impacts will be exacerbated during the most extreme events, particularly under high-emission pathways. Cyclones can be one of the main factors for extreme dust transport events in the region, contributing to elevated concentrations and long-range transport, enhancing and expanding the exposure of the population and associated health effects. The human health effects of dust storms range from respiratory disorders (including asthma, tracheitis, pneumonia, allergic rhinitis and silicosis), to cardiovascular disorders, such as strokes, conjunctivitis, skin irritations, meningococcal meningitis, valley fever, diseases associated with toxic algal blooms, and mortality and injuries related to transport accidents. Serious risks to human health can be posed by both chronic exposure and short-term elevated concentrations of airborne dust. In the Eastern Mediterranean region premature mortality attributable to chronic $PM_{2.5}$ exposure is mainly related to natural aeolian dust processes. In the so-called "dust belt" from North Africa across the Middle East and South Asia to East Asia, the fraction of the cardiopulmonary deaths caused by atmospheric desert dust can reach 15–50%. In several Mediterranean countries, including Cyprus, Italy, Israel and Spain, cardiovascular and respiratory admissions and mortality rates are found enhanced during dust events. While the Mediterranean Cyclones that drive most dust storms in the region could be less frequent in a warmer world, drier soils (e.g., the dried lake beds lying in topographically-low basins) will be highly susceptible to aeolian erosion, therefore, dust emissions in the region, including sources in the Middle East, could be increased.

Temperature: The direct and indirect health implications due to extreme precipitation and wind are more widespread; nevertheless, extremely cold temperatures, sometimes driven or favoured by Mediterranean cyclones, can also affect the health and well-being of the region's population. Besides the overall mild temperatures during the cold season, excess winter mortality and morbidity are observed in several Mediterranean countries. This includes increased risk of all-cause mortality, cardiovascular mortality and respiratory mortality in extreme cold events. However, this is highly correlated to socio-economic factors such as energy poverty or building standards, while it is also related to influenza epidemics. Most future assessments for the region focus on the health impacts of heat extremes, as a warmer world implies an apparent decline in cold-wave-related mortality. Although cold-temperature extremes in the region are mostly related to polar air mass outbreaks and anticyclonic activity that favours persistent north flows, extratropical low-pressure systems that are associated with pronounced upper-level cold troughs can drive severe cold weather. Such settings occasionally provide the necessary elements for heavy precipitation, which, given the low temperatures, can result in intense snowfall or freezing rain.

III.2. Future suitability of Asian tiger mosquito

Climate change can influence the transmission of vector-borne diseases (VBDs) by altering the habitat suitability of insect vectors. This is mainly controlled by increases in ambient air temperature and changes in the hydrological cycle. For example, the Asian tiger mosquito (*Aedes albopictus*) is native to Southeast Asia's tropical and subtropical areas; however, in the past few decades, this species has spread to many countries through the international transport of goods and increased travel. It is of great epidemiological importance since it can transmit viral pathogens and infectious agents that cause chikungunya, dengue fever, yellow fever and various forms of encephalitis (Proestos et al. 2015). There is some evidence supporting the role of *Ae. albopictus* in the transmission of the Zika virus, which is primarily transmitted by the related *Ae. aegypti*. The Asian tiger mosquito is now listed as one of the top 100 invasive species by the Invasive Species Specialist Group (http://www.issg.org/).

According to the European Centre for Disease Prevention and Control (ECDC; https://ecdc.europa.eu/), *Ae. albopictus* has been established in the following European areas: Albania, Bosnia & Herzegovina, Bulgaria, Croatia, France (including Corsica), Georgia, Germany, Greece, Hungary, Italy (including Sardinia, Sicily, Lampedusa, and other islands), Malta, Monaco, Montenegro, Romania, Russia, San Marino, Slovenia, Spain, Switzerland, Turkey and Vatican City. The presence of invasive vectors, such as the Asian tiger mosquito, is expected to significantly affect several socio-economic sectors (incl. tourism and public health). Therefore, investigating potential changes to its suitability and understanding how this is impacted by climate and environmental change is of outmost importance.

Recently, to assess the impact of climate change on the spread of such vectors, we applied the methodology described in Proestos et al. (2015). The multi-criteria decision support vector distribution model has been employed to estimate the regional habitat suitability maps for the broader Euro-Mediterranean regions (González, 2021). The mosquito habitat suitability model combines seven meteorological indices based on field observations, extensive literature review and expert knowledge. The model serves as a tool to explore and identify the geographical areas that can potentially sustain the thriving of the mosquito in recent and future periods considering climate change scenarios. The seven empirical criteria obtained from regional climate model outputs to estimate the environmental suitability for the Asian tiger mosquito are given below.

1. The annual average precipitation is at least 200 mm.
2. The annual average temperature is higher than 8.0°C.

3. In January of the Northern Hemisphere (NH) (July of the Southern Hemisphere) minimum temperature is above -4.0°C.
4. The summer maximum temperature does not exceed 40.0°C.
5. At least 60 days have measurable rainfall (greater than 1 mm).
6. The summer RH is at least 30% and
7. the winter RH is 50% or higher.

For this assessment, we followed a fuzzy-logic methodology based on sigmoidal membership functions. The latter are continuous (smooth) functions that can be used to express the degree of suitability of a certain meteorological variable around a threshold. After rescaling each of the seven habitat variables using the sigmoidal functions, we define the Habitat Suitability Index (HSI), which is a measure of the possible spatial (habitat) distribution of the Asian tiger mosquito. A detailed description of the methodology can be found in Proestos et al. (2015). HSI takes values from 0 to 100 with higher values indicating higher suitability. An interpretation of the HSI values is presented in Table 1. The meteorological parameters needed to define the suitability of the Asian tiger mosquito were derived from state-of-the-art EURO-CORDEX regional climate simulations. These data have a horizontal resolution of 12.5-km (0.11 degrees).

Table 1. Interpretation of the Habitat Suitability Index (HSI) values for *Ae. Albopictus.*

Aedes Albopictus Habitat Suitability Index	
80 - 100	High Suitability
60 - 80	Medium Suitability
40 - 60	Low Suitability
< 40	No Suitability

An example of the habitat suitability projections for two Eastern Mediterranean islands (Cyprus and Crete), for different periods in the 21st century and under different emission scenarios is presented in Figure 13.

For the case of Cyprus, for the historical period the simulated climate conditions, verified by observations, indicate a medium suitability according to our definition (HSI values of 68.7). This is expected to increase slightly in a future of substantial climate change mitigation (pathway RCP2.6). On the contrary under business-as-usual RCP8.5 suitability is expected to decrease. For a large part of the island (mainly inland) the future climatic conditions will likely be unfavorable for the Asian tiger mosquito. At the same time, high suitability is mostly simulated over the mountainous areas of Troodos (Figure 13 – top panels) where summer temperatures are not expected to exceed the 40°C threshold (not shown).
For the Greek island of Crete, the environmental conditions are also already favourable for the establishment of *Ae. Albopictus* (Figure 13 – bottom panels). Future regional simulations under RCP2.6 suggest a slight increase in the values of HSI. In agreement with the future trends for Cyprus, pathway RCP8.5 implies a decrease in the habitat suitability. This is more evident in the central inland regions and in the southwest parts of the island and is related to the strong warming projected for the eastern Mediterranean under this pathway.
More information on the methodologies and detailed results for each European island assessed are available in León et al., 2021.

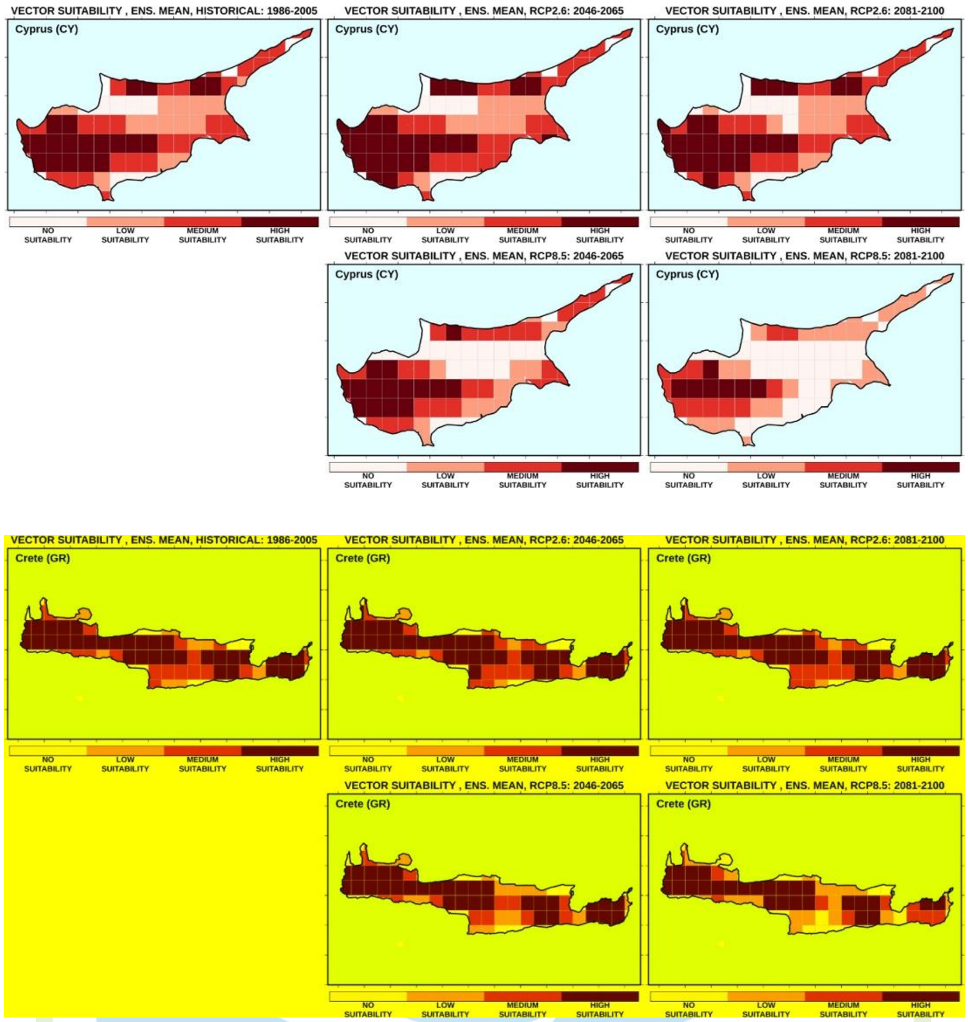

Figure 13. Historical and future suitability maps for *Aedes albopictus* in Cyprus (top panels) and Crete (bottom panels), based on the EURO-CORDEX multi-model ensemble.

III.3. Machine learning approach to habitat suitability

We have also developed a machine learning approach for predicting *Aedes albopictus* (invasive Asian tiger mosquito) habitat suitability and projecting its change until the end of the century.
By combining Random Forest and XGBoost binary classifiers, we developed an ensemble machine learning model, and trained it using global vector surveillance data. Instead of using point presence and background/pseudo-absence data, we employed high-quality longitudinal surveillance data from the following data sources across Europe and the United States of America:
- VectorBase PopBio (MapVEu tool) population abundance dataset.
- *Aedes albopictus* surveillance dataset of Emilia-Romagna (2008-2012).
- Surveillance data from our collaborators from Hungary, Slovenia, Serbia, and Bulgaria.
- Data from the *Aedes* Challenge Project organised by the Centre of Disease Control (CDC).

We harmonised and gridded the longitudinal data using a regular grid of 0.25° spatial resolution (1440×720 grid cells). We assigned present (1) and absent (0) classes for each month, and used 90% of the data for training. The geospatial extent of the training dataset and the representation of each month are shown in Figure 14.

We obtained land use data from the Land Use Harmonization (LUH2) program, human population density matching SSP245 and SSP585 scenarios from Jones and O'Neil (2016), and included climate features, such as daily minimum, maximum, and average temperature, total precipitation and relative humidity, from the NASA Earth Exchange (NEX) Global Daily Downscaled Projections (GDDP) (NEX-GDDP-CMIP6).

We integrated a Random Forest classifier and an XGBoost classifier into a binary classification ensemble model by allowing each to perform independent predictions and choosing the one with the highest probability sum over each predicted class.

We projected present and future potential habitat suitability following the two IPCC RCP scenarios, the “stabilization” scenario SSP245 and the “business-as-usual” scenario SSP585, and obtained the average of 9 climate models (ACCESS-ESM1-5, EC-Earth3, GFDL-CM4, FGOALS-g3, INM-CM4-8, INM-CM5-0, MIROC6, MRI-ESM2-0, and NorESM2-MM).

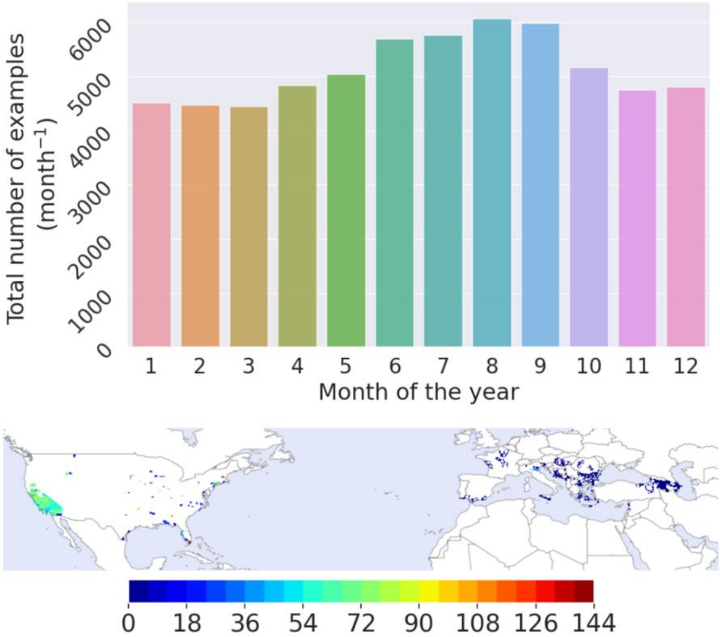

Figure 14. Monthly distribution (top) and the geospatial extent (bottom) of the cases included in the training set. The colour bar indicates the number of examples for each grid cell for the bottom panel.

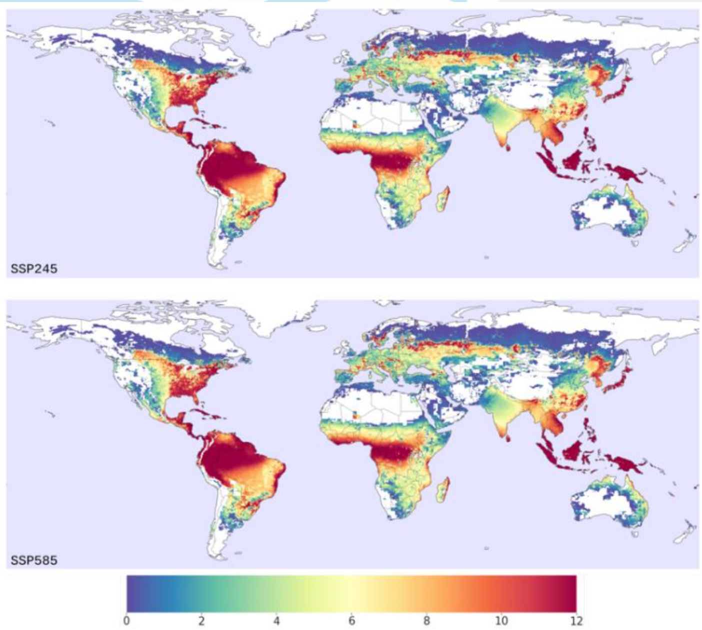

Figure 15. Predicted *Ae. albopictus* habitat suitability in terms of months predicted as suitable by the ensemble model for the early part of the century (2020–2025) according to two IPCC scenarios.

We found that, regardless of the IPCC scenario, we expect an increase in the number of months predicted as suitable across all the latitudes throughout the 21st century. Especially, our results corroborate the widely reported prediction of polewards expansion of suitable habitats for *Aedes albopictus* as a result of climate and land use changes until the end of the century (Figure 16).

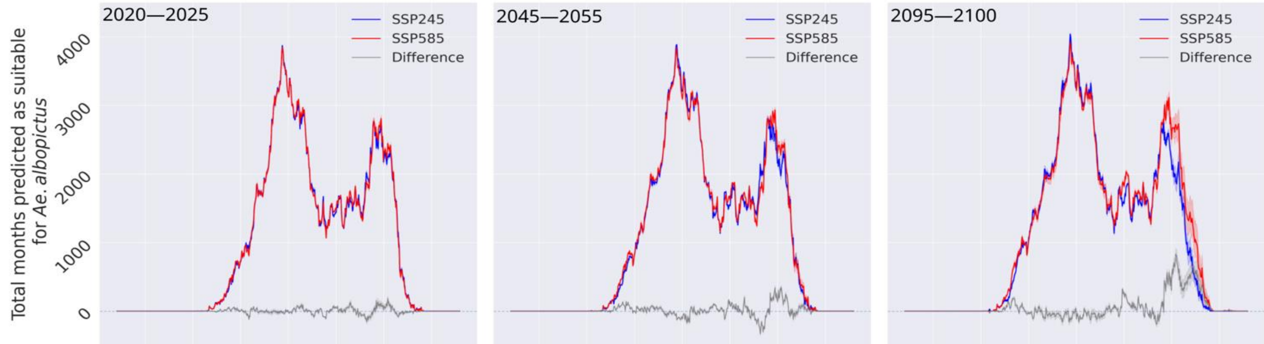

Figure 16. Latitude profiles (sum of months designated as suitable over latitudes) for the total number of months predicted as suitable by the model, and transitional changes between early to mid, end of century, and mid to end of century periods.

We found that approximately five billion people inhabit areas suitable for the establishment of *Ae. albopictus* in the year 2020. We projected a dramatic increase in the number of people at risk for the mid-century time period (2045–2055) for both IPCC scenarios (up to 1.5 billion for SSP245 and 1.1 for SSP585). We found that SSP585 consistently leads to a more moderate increase, which manifests into a steep difference between the two scenarios for the end-of-century time period (2095–2100). This striking difference is mainly attributed to the projected adverse effect of the business-as-usual scenario on human population at the end of the 21st century. Even though the total population in the SSP585 scenario is projected to fall below the current level, an additional 0.4 billion people are predicted to be at risk of *Ae. albopictus*-borne diseases by the end of century, as a result of suitable habitat expansion. **A manuscript of this work is published in the Insects journal (**in the Special Issue of Climate Sensitive Ecological and Dynamical Models of Insects), *Georgiades et al. (2023)* "in the Special Issue of Climate Sensitive Ecological and Dynamical Models of Insects" (https://doi.org/10.3390/insects14050447).

III.4. Continental population dynamics modelling for the Asian tiger mosquito

As an alternative approach to modelling habitat suitability, and to enable predicting change in abundance and activity, we developed a climate- and environment-driven population dynamics model of *Aedes albopictus* with extensive geospatial applicability. The foundation of the model is the age- and stage-structured population dynamics model developed by Erguler et al. (2016). We extended this model with the framework of adaptive and accumulative development (see the next section), and revised and improved the environmental dependency components, such as the dependence of diapause and egg hatching on day length and temperature, and the dependence of the carrying capacity on rainfall, human activities, and land cover.

We employed the longitudinal datasets from VectorBase PopBio (the MapVEu tool as above) and AIMSurv (the first pan-European harmonized surveillance of *Aedes* invasive mosquito species of relevance for human vector-borne diseases). We note that members of the IPD joined the AIMSurv surveillance network and became the first to discover the presence of *Aedes albopictus* in Cyprus (Christou et al, 2023) "First record of the invasive Asian tiger mosquito Aedes albopictus in Cyprus based on information collected by citizen scientists" (https://doi.org/10.52004/JEMCA2022.0008).

To employ for the project, we extracted all publicly available longitudinal data, filtered for the duration of observations (observed for at least three consecutive months), gridded with respect to the regular grid of 0.25° spatial resolution, and presented in Figure 17.
Using the entire dataset (grouped into 136 grid cells), we estimated a theoretical index of carrying capacity, as a function of land cover and human population density, and used this to drive the breeding site availability (BSA) component of the population dynamics model. We assumed that the BSA also changes with rainfall, evaporation, and vector management practices.

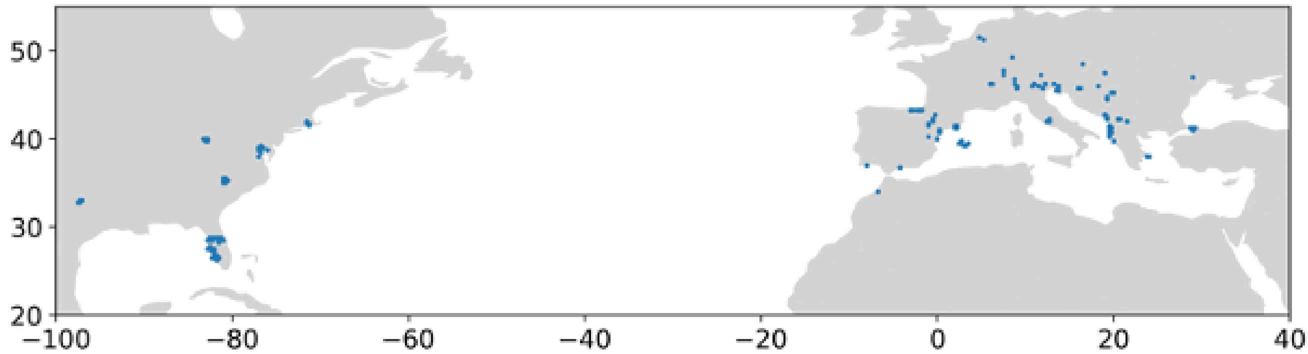

Figure 17. The gridded longitudinal data from Europe and the United States of America.

We selected a small subset of the longitudinal data (8 grid cells from various locations) to performed Bayesian inference on all model parameters (priors of environmental dependencies were derived from the literature). As a result, we achieved geospatial applicability over Europe and North America, and corroborated that temperate northern territories are becoming increasingly suitable for *Aedes albopictus* establishment, while neighbouring southern territories become less suitable, as climate continues to change (Figure 19). We identified potential hotspots over Europe and North America by employing the combination of vector abundance and activity as a proxy to pathogen transmission risk. A manuscript of this work is in preparation.

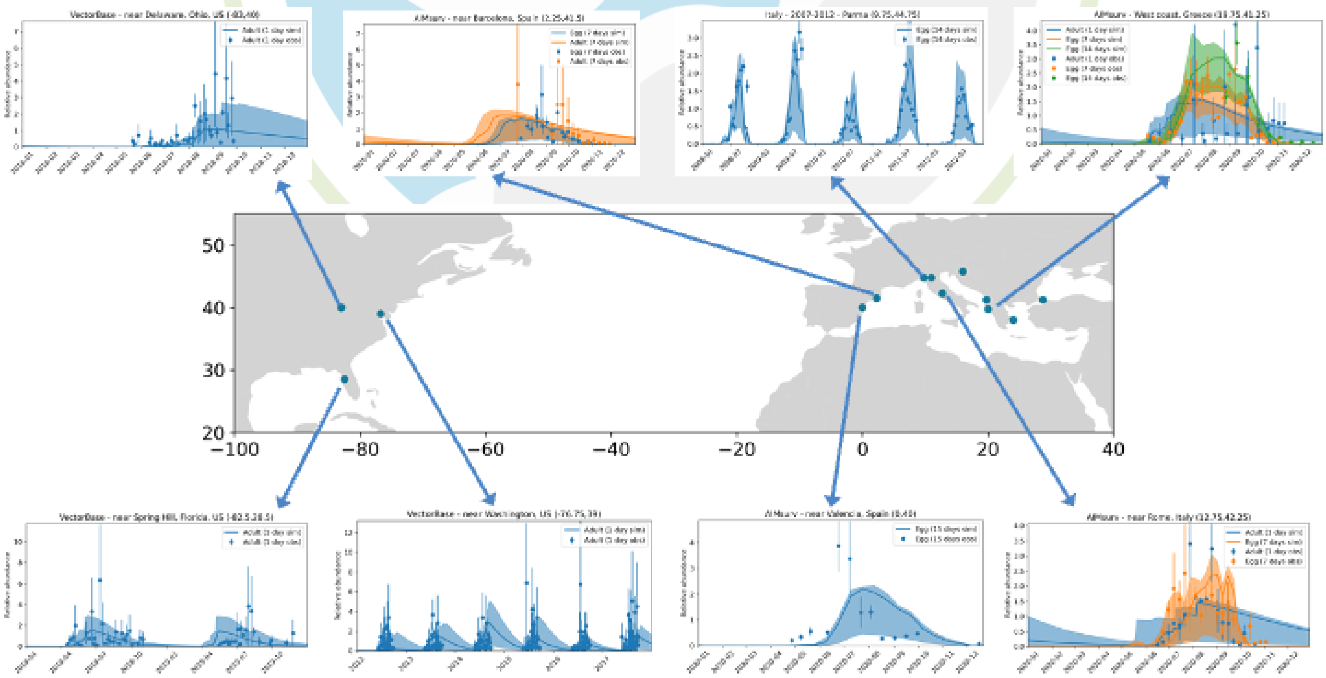

Figure 18. Model fit to the longitudinal data from different locations.

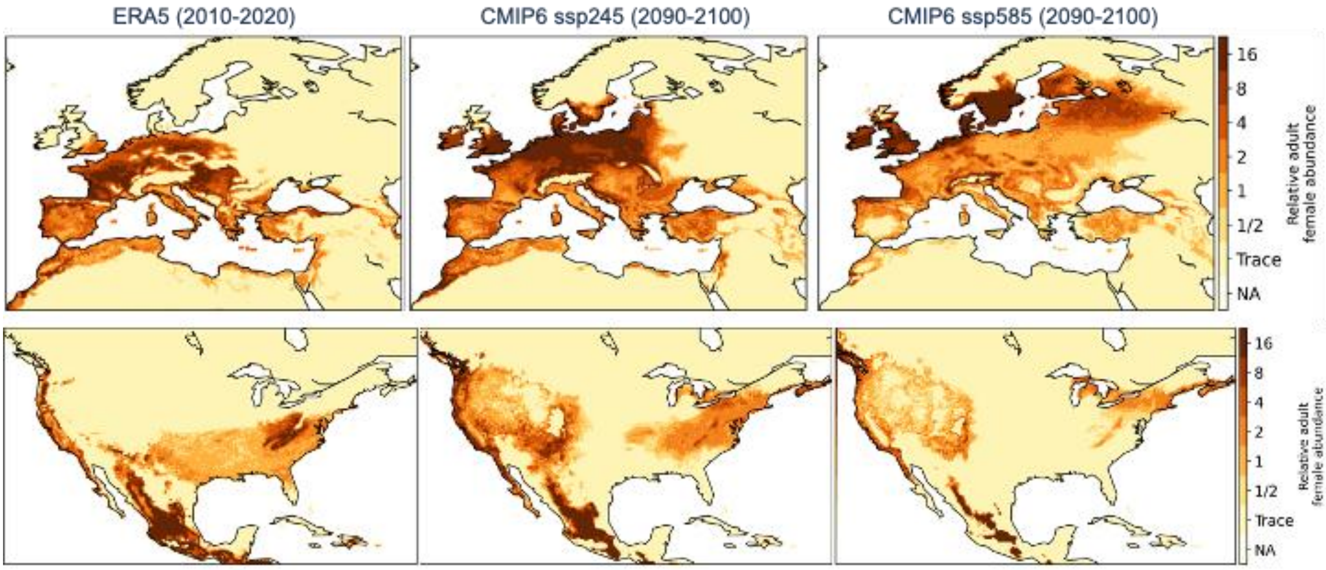

Figure 19. Projected poleward shift of average *Aedes albopictus* abundance according to CMIP6 - ACCESS-CM2 model under two IPCC scenarios.

III.5. Modelling insect physiology under variable conditions

The work presented here has been recently published as *Erguler et al. (2022)* ”A dynamically structured matrix population model for insect life histories observed under variable environmental conditions” (https://doi.org/10.1038/s41598-022-15806-2).

It addresses the inadequacy of the current mathematical and computational tools to model the dynamics of populations that depend on constantly varying external conditions, such as climate and other environmental factors. To address this gap, we represented life processes (survival, development, etc.) as renewal processes with a dynamic probability of event arrival. While each renewal event corresponds to a fraction of completeness of a life process, individuals with identical fractions are grouped together to form a pseudo-stage-structured population. We developed an algorithm to facilitate the dynamic handling of the pseudo-stages, allow for intrinsic stochasticity, and accommodate variable interarrival times. We implemented the algorithm in C and distributed it under the GPL 3.0 license on the GitHub repository (Erguler, 2021) as an extension to the age- and stage-structured population dynamics model of Erguler (2020).

To demonstrate the advantage of this method, we inferred the temperature dependence of development and mortality of *Culex pipiens* biotype *molestus* (the common house mosquito capable of transmitting the West Nile virus). We used a generic insect development model constructed using our sPop2 framework, and calibrated it with life tables observations (development and survival of each stage) performed under variable conditions (outside in the garden) throughout the year. As a result, we identified the dependencies accurately with the range of temperatures observed, and also found that the larva development of the species depends on day length (Figure 20). Using the inferred dependencies, we estimated the expected development time, survival, and the time to the first emergence of adults throughout the year in Petrovaradin, Serbia (Figure 21).

The methods introduced can be used to accurately characterise a wide range of external drivers without the need to collect large amounts of data. Our approach complements the analytical and experimental methods needed for developing predictive large-scale climate-driven models for many insect species, such as those important for disease transmission, species conservation, and forensic investigation.

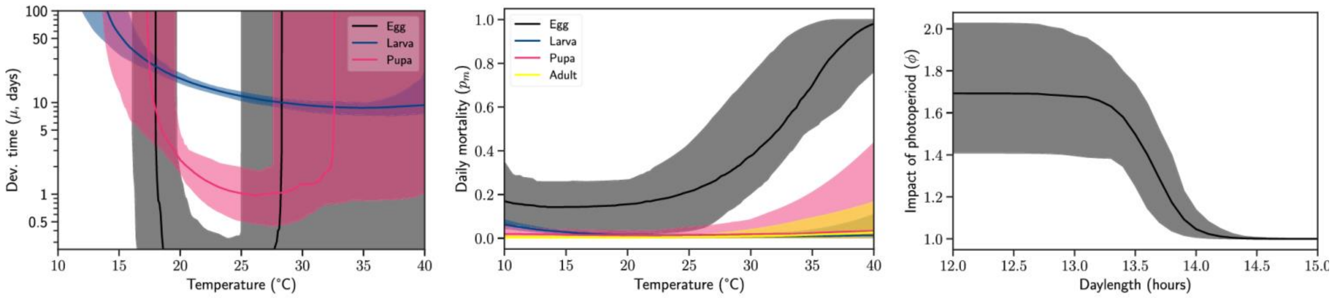

(a) Mean development time (days) (b) Daily mortality (fraction) (c) Fractional extension of development time

Figure 20. Environmental dependency of *Cx. pipiens* development and mortality inferred from semi-field life table experiments. Solid lines represent the median and shaded areas represent the 90% range.

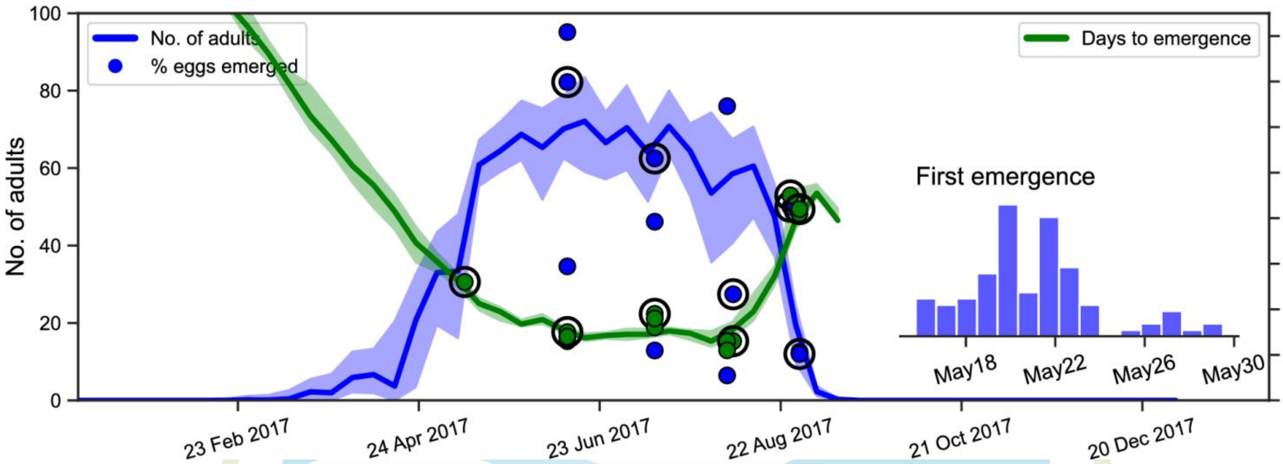

Figure 21. Annual development profile of *Cx. pipiens* in Petrovaradin, Serbia, in 2017.

III.6. Climate change, human security and conflicts

Climate change can challenge human security by (a) undermining livelihood, culture and human rights, (b) increasing migration, and (c) indirectly influencing armed conflict.
In particular, **our work** showed that Climate-driven limitations in water and other resources (e.g., due to prolonged drought events) are found to directly or indirectly trigger or augment disputes and conflicts in the EMME region (Zittis et al., 2022) “Climate Change and Weather Extremes in the Eastern Mediterranean and Middle East” (https://doi.org/10.1029/2021RG000762).
However, their relative importance, in comparison to other causes, remains controversial. The projected climate changes will likely further increase regional energy demand and may lead to reduced crop yields. Such impacts will increase the existing social contrasts between populations in the region, potentially increasing food insecurity, prices and contributing to malnutrition. Such changes can drive political tensions and instabilities that may ultimately lead to conflicts and humanitarian crises. Regional economic, political, demographic, and social drivers, as well as climate-related environmental stressors (e.g., droughts, extreme heatwaves, or vector-borne diseases spread), could contribute to migration flows, with climate change acting as a push factor. The scale and geographic scope of such population displacements could be one of the greatest human rights challenges of our time. Migration is not solely driven by climate change but by a combination of environmental, socio-economic, cultural and political factors. Historically, in the arid to semi-arid areas of the Middle East, such changes have been drivers of human settlement and population migrations. In historical times, migration may have been the only adaptation option. The additional stress from climate change to prevailing conflicts between countries

and populations may have dire consequences for weakened populations, also in refugee camps, exposing them to high risks and contributing to migration, with the associated suffering from malnutrition, poor sanitation and a lack of medical and mental support infrastructure.

Assessing such population and social dynamics under future scenarios is a challenging task. It requires multi-disciplinary expertise and interactions between physical sciences (climate and atmospheric modelling, extreme events analysis, etc.) and also social sciences (e.g., sociological, political, and economic sciences). The MedECC network (Mediterranean Experts on Environmental and Climate Change) launched an international initiative on understanding the potential linkages between environmental and climate change, conflicts, human migration and eventually public health and wellbeing in the broader Mediterranean region. This special report (https://www.medecc.org/medecc-reports/medecc-special-reports-2021-2023/) is currently in preparation (external review stage) and is expected to be released this year. EMME-CARE contributes as an expert on regional climate change and future projections.

IV. Future plans

Some work is currently ongoing while several other studies are planned that build upon the research presented in this Deliverable D7.2. We present an overview here of this work (related to Task 7.2):

- Future projections of meteorological and hydrological drought risk for better understanding projections of water security for the EMME region.
- Artificial Intelligence methods for quantifying historical and future trends of the Urban Heat Island effect for the Middle East and North Africa region, and the associated impact to human health.
- Better understanding food security hazards for the region, by computing projections of climate indices known to negatively impact agriculture and animal farming.
- Assess the impacts of climate change on human security, conflicts and migration in the broader Mediterranean region.
- Future projections of the compound effects from poor air quality and heat stress for Cyprus and Greece, based on observed mortality and morbidity data
- High resolution future projections of mortality hazard, exposure and vulnerability for the EMME region as a function of heat-stress.

V. Projects related to Task 7.2

The list below consists of relevant funded and upcoming research projects, whose objectives are aligned with EMME-CARE goals and have in part contributed to the abovementioned research activities (Task 7.2):

- LIFE-SIRIUS: A System for Integrated Environmental Information in Urban areaS - LIFE Programme European Union project LIFE21-GIE-EL-LIFE-SIRIUS/10107436.
- SOCLIMPACT - DownScaling CLImate imPACTs and decarbonisation pathways in EU islands, and enhancing socioeconomic and non-market evaluation of Climate Change for Europe, for 2050 and beyond. EU Horizon 2020 Research and Innovation Programme, Grant agreement number 776661.
- MedCyclones: The European network for Mediterranean cyclones in weather and climate. COST Action CA19109.
- VEClim: Climate-driven vector-borne disease risk assessment, funded by Wellcome Trust, UK, as part of Digital Technology Development Awards in Climate Sensitive Infectious Disease Modelling.
- PREVENT: Improved predictability of extremes over the Mediterranean from seasonal to decadal timescales. EU Horizon Europe (2023-2026)

VI. References

Burnett, R.T., Pope, C.A. III, Ezzati, M., Olives, C., Lim, S.M., Mentha, S., Shin, H.H., Singh, G., Hubbell, B., Brauer, M., et al. (2014). An integrated risk function for estimating the global burden of disease attributable to ambient fine particulate matter exposure. Environmental Health Perspectives, DOI: https://doi.org/10.1289/ehp.1307049.

Burnett R., et al. (2018) Global estimates of mortality associated with long-term exposure to outdoor fine particulate matter. Proceedings of the National Academy of Sciences. DOI: 10.1073/pnas.1803222115.

Chowdhury S., Haines A., Klingmüller K., Kumar V., Pozzer A., Venkataraman C., Witt C and Lelieveld J. (2021) Global and national assessment of the incidence of asthma in children and adolescents from major sources of ambient NO_2. Environmental Research Letters, DOI: 10.1088/1748-9326/abe909.

Christou M, Lippert S., Weigand A., Angelidou I., Athanasiou K. C., Demetriou J., Schaffner F. and Martinou A. F. (2023). First record of the invasive Asian tiger mosquito Aedes albopictus in Cyprus based on information collected by citizen scientists. Journal of the European Mosquito Control Association. DOI: https://doi.org/10.52004/JEMCA2022.0008.

Cohen, A.J., Brauer, M., Burnett, R.T., Anderson, H.R., Frostad, J., Estep, K., et al. (2017). Estimates and 25-year trends of the global burden of disease attributable to ambient air pollution: an analysis of data from the Global Burden of Diseases Study 2015. The Lancet. DOI: 10.1016/S0140-6736(17)30505-6.

Erguler K., Smith-Unna S. E., Waldock J., Proestos Y., Christophides G. K., Lelieveld J. and Parham P. E. (2016). Large-Scale Modelling of the Environmentally-Driven Population Dynamics of Temperate Aedes albopictus (Skuse). PLOS ONE. DOI: https://doi.org/10.1371/journal.pone.0149282.

Erguler K. (2020) sPop: Age-structured discrete-time population dynamics model in C, Python, and R [version 3; peer review: 2 approved]. F1000Research, 7:1220 DOI: https://doi.org/10.12688/f1000research.15824.3.

Erguler. (2021). kerguler/sPop2: sPop2: a dynamically-structured matrix population model (v2.1). Zenodo. DOI: https://doi.org/10.5281/zenodo.5788377.

Erguler K., Mendel J., Petrić D. V., Petrić M., Kavran M., Demirok M. C., Gunay F., Georgiades P., Iten B. and Lelieveld J. (2022). A dynamically structured matrix population model for insect life histories observed under variable environmental conditions. Scientific Reports. DOI: https://doi.org/10.1038/s41598-022-15806-2.

Georgiades P., Proestos Y., Lelieveld J. and Erguler K. (2023). Machine Learning Modeling of Aedes albopictus Habitat Suitability in the 21st Century. Insects. DOI: https://doi.org/10.3390/insects14050447.

González Y. E. L., Garcia C., Hernández M.M.G. and Leon,C. J.. (2021). Downscaling climate change impacts, socio-economic implications and alternative adaptation pathways for islands and outermost regions. Final report for the SOCLIMPACT project. DOI: https://doi.org/10.5281/zenodo.5141549.

Hajat S., Proestos Y. Araya-Lopez J., Economou T and Lelieveld J. (2023) Current and future trends in heat-related mortality in the MENA region: a health impact assessment with bias-adjusted statistically downscaled CMIP6 (SSP-based) data and Bayesian inference. The Lancet Planetary Health. DOI: https://doi.org/10.1016/S2542-5196(23)00045-1.

Himics M., E. Giannakis, J. Kushta, J. Hristov, A. Sahoo, and I. Perez-Dominguez, 2022, Co-benefits of a flexitarian diet for air quality and human health in Europe, Ecological Economics, ECOLEC-D-20-00293R2, https://doi.org/10.1016/j.ecolecon.2021.107232 , 2022.

Khodayar S., Kushta J., Catto J., Dafis S., Davolioc S., Ferrarin C., Flaounas E., Groenemeijer P., Hatzaki M., Hochman A., Kotroni V., Landa J, Láng-Ritter I., Lazoglou G., Liberato M., Miglietta M.M., Papagiannaki, K. Patlakas P., Stojanov R., Zittis G. (2023). Socio-economic impacts of Mediterranean cyclones in a changing climate. (submitted).

Kushta J, Paisi N, Gon HD, Lelieveld J (2021) Disease burden and excess mortality from coal-fired power plant emissions in Europe. Environ Res Lett 16:045010. https://doi.org/10.1088/1748-9326/ABECFF.

Lelieveld J., Helleis F., Borrmann S., Cheng Y., Drewnick F., Haug G., Klimach T., Sciare J., Su H. and Pöschl U. (2020) Model calculations of aerosol transmission and infection risk of COVID-19 in indoor environments. International Journal of Environmental Research and Public Health, DOI: https://doi.org/10.3390/ijerph17218114.

León C., et al. (2021) Downscaling climate change impacts, socio-economic implications and alternative adaptation pathways for islands and outermost regions. Madrid: McGraw¬Hill. https://doi.org/10.5281/zenodo.5141549

Markandya A. and Wilkinson P. (2007). Electricity generation and health, The Lancet, DOI: https://doi.org/10.1016/S0140-6736(07)61253-7.

Paisi N, et al. (2023) Modeling of carbonaceous aerosols for air pollution health impact studies in Europe, under review at Air Quality Atmosphere and Health, Special Issue: HARMO21-Harmonisation within Atmospheric Dispersion Modelling for Regulatory Purposes.

Proestos Y., Christophides G.K., Ergüler K., et al. (2015) Present and future projections of habitat suitability of the Asian tiger mosquito, a vector of viral pathogens, from global climate simulation. Philosophical Transaction of the Royal Society B. DOI: 10.1098/rstb.2013.0554.

Venter Z. S., Aunan K., Chowdhury S. and Lelieveld J. (2021). Air pollution declines during COVID-19 lockdowns mitigate the global health burden. Environmental Research, DOI: https://doi.org/10.1016/j.envres.2020.110403.

Venter Z. S., Aunan K., Chowdhury S. and Lelieveld J. (2020). COVID-19 lockdowns cause global air pollution declines. Proceedings of the National Academy of Sciences. DOI: https://doi.org/10.1073/pnas.2006853117.

Zittis G., Almazroui M., Alpert P., Ciais P., Cramer W., Dahdal Y., Fnais M., Francis D., Hadjinicolaou P., Howari F., Jrrar A., Kaskaoutis D., Kulmala M., Lazoglou G., Lin X., Mihalopoulos N., Rudich Y., Sciare J., Stenchikov G., Xoplaki E., Lelieveld J. (2022) Climate change and weather extremes in the Eastern Mediterranean and Middle East. Reviews of Geophysics. DOI: https://doi.org/10.1029/2021RG000762BNM.